

Stony Brook University



OFFICIAL COPY

The official electronic file of this thesis or dissertation is maintained by the University Libraries on behalf of The Graduate School at Stony Brook University.

© All Rights Reserved by Author.

Isotopy Invariants of Immersed Surfaces in a 4-manifold

A Dissertation Presented

by

Luoying Weng

to

The Graduate School

in Partial Fulfillment of the

Requirements

for the Degree of

Doctor of Philosophy

in

Mathematics

Stony Brook University

December 2011

Stony Brook University

The Graduate School

Luoying Weng

We, the dissertation committee for the above candidate for the Doctor of Philosophy degree, hereby recommend acceptance of this dissertation.

Oleg Viro - Advisor

Professor, Department of Mathematics

Alexander Kirillov, Jr. - Chairperson of Defense

Associate Professor, Department of Mathematics

Olga Plamenevskaya

Assistant Professor, Department of Mathematics

Alexander Shumakovitch

Assistant Professor, Department of Mathematics, George Washington
University

This dissertation is accepted by the Graduate School.

Lawrence Martin

Dean of the Graduate School

Abstract of the Dissertation

**Isotopy Invariants of Immersed
Surfaces in a 4-manifold**

by

Luoying Weng

Doctor of Philosophy

in

Mathematics

Stony Brook University

2011

In this this dissertation we introduce an isotopy invariant of generically immersed surfaces in some 4-manifold. The construction is based on Khovanov homology and its variants in the same way as the construction of Turaev-Viro module of a 3-manifold with infinite cyclic covering relies on TQFT. The invariant is first constructed for generically immersed surfaces in $S^3 \times S^1$ using the functoriality of Khovanov homology, and is generalized

by using new versions of Khovanov homology. Moreover, it is also generalized to surfaces generically immersed transversal to a standardly embedded S^2 in S^4 . Examples are studied to illustrate the strength and weakness of this invariant.

To my family

Contents

List of Figures	ix
Acknowledgements	xii
1 Introduction	1
2 Khovanov Homology	4
2.1 Khovanov Chain Complex	4
2.2 Link Cobordisms and Movie Moves	7
2.3 Two Categories and Khovanov Homology	10
3 Immersed Link Cobordisms and Khovanov Homology	13
3.1 Immersed Link Cobordisms	13
3.2 Extend Khovanov Homology to a New Category	15
4 Framed Khovanov Homology	21
4.1 Framed links and diagrams	21
4.2 Normal Euler Number	23

4.3	Framed Khovanov homology	24
4.4	Categories of framed links and their diagrams	32
5	The Construction of the New Invariant	34
5.1	The construction	34
5.2	An isotopy invariant	40
6	Examples	46
6.1	Surfaces Obtained by Planer Isotopy	53
6.1.1	Product Surfaces	53
6.1.2	Surfaces Obtained by Rotations	53
6.2	Surfaces Obtained by Reidemeister Moves	62
6.2.1	Klein Bottle	62
6.2.2	Interchange component of Whitehead link	65
6.2.3	Second and Third Reidemeister moves	65
6.3	Examples using surgeries	72
7	Generically Immersed Surfaces in S^4	78
	Bibliography	81
A	Calculations on Extra Movie Moves	83
B	A Program to Compute Khovanov Homology	87
B.1	Introduction to KhoHo.	87
B.2	Extensions to KhoHo.	90

C Some Computational Results	104
D Calculations on the Third Reidemeister Moves	107

List of Figures

2.1	Smoothings of a crossing according to markers	4
2.2	Third Reidemeister move in changing discs	9
2.3	Carter and Saito's movie moves.	12
3.1	Extra Movie Moves	16
4.1	Local picture for a framing	22
4.2	Decoration framings	22
4.3	A framed trefoil	23
4.4	The first framed Reidemeister moves	25
4.5	Twist annihilation move	25
4.6	Twist penetration move	25
4.7	0,2-surgeries.	29
4.8	1-surgery along two compatible framed arcs	29
4.9	1-surgery along two non-compatible framed arcs	30
5.1	Composition of cobordisms	37
5.2	$Kh_s(W)$ is an isomorphism	38

5.3	$Kh_s(F_0) \cong Kh_s(W)^{-1} \circ Kh_s(F'_0) \circ Kh_s(W)$ in case (1)	39
5.4	$Kh_s(F_0) \cong Kh_s(W)^{-1} \circ Kh_s(F'_0) \circ Kh_s(W)$ in case (2)	40
5.5	A cobordism induced by the isotopy of diffeomorphisms	42
5.6	Pull back cobordism in \tilde{F}	43
5.7	New cobordisms under ambient isotopy ϕ_t .	44
6.1	Rotate a trefoil knot clockwise by 120 degree	47
6.2	Knot(8,18)	47
6.3	Orientation flipping move F_k with positive twist	48
6.4	Interchange of components of Whitehead link	48
6.5	Arc sliding	49
6.6	A surface F obtained by Reidemeister moves and surgeries	50
6.7	A cobordism with a double point	50
6.8	Surface obtained by non-orientation-preserving surgery	51
6.9	Notations for surgeries	52
6.10	Enhanced states of Trefoil knot	55
6.11	First Reidemeister move with positive kink	62
6.12	Orientation flipping move F'_k with negative twist	63
6.13	First Reidemeister move with negative twist	64
6.14	Chain maps induced by the second Reidemeister move.	67
6.15	Compare of R_3 maps(1)	69
6.16	Compare of R_3 maps(2)	70
B.1	Diagram of trefoil knot	88

C.1	Borromean Ring	104
C.2	Knot(10,123)	105
D.1	Slide over a crossing	108
D.2	Slide under a crossing	111
D.3	Slide over or under	114

Acknowledgements

I am heartily thankful to my advisor, Oleg Viro, whose encouragement, guidance and support from the initial to the final level enabled me to develop an understanding of the subject. He always explained abstract and difficult ideas in a geometric way that I can understand easily. It was really a great experience to see his ways of understanding and solving mathematical problems.

I would also like to thank Eugene Gorsky, Lowell Jones, Alexander Kirillov Jr., Olga Plamenevskaya, Dennis Sullivan and Aleksey Zinger for helpful conversations on mathematics. I would like to show my gratitude to Alexander Shumakovitch for driving all the way from Washington D.C to Stony Brook for my defense. I am greatly indebted to all faculty for the wonderful courses they have taught during my study in Stony Brook.

Special thanks go to Somnath Basu and Weixin Guo for their helpful discussions in various topics in mathematics, and Xiaojie Wang for his help in my daily life. I am also grateful to Mark Hughes for being the first listener of my practice defense presentation and Eitan Chatav for pointing out mistakes in my thesis draft.

I am also indebted to my many of my colleagues to support me in Stony Brook: Andrew Bulawa, Xiaojun Chen, Ying Chi, Ning Hao, Li Li, Yinghua Li, Ritwik Mukherjee, Zhiyu Tian, Dezhen Xu and Jason Zou.

Last and most importantly, I owe my deepest gratitude to my family.

Dad, Mom and my dear brother, thank you for your love, understanding and continuous support. Any Jingyu, my dear girlfriend, thank you for being so supportive all the time.

Chapter 1

Introduction

Khovanov homology has been proved to be functorial up to sign by Jacobson [4] and Bar-Natan [1]. One can try to use this functoriality for defining an invariant of closed surface smoothly embedded in \mathbb{R}^4 . The most straightforward approach was to consider the surface as an oriented cobordism between two empty links. For simple grading reasons, this invariant is trivial for surfaces with non-zero Euler characteristic. For surfaces homeomorphic to torus this invariant was proved to be trivial by Rasmussen [9] and Tanaka [12].

In this dissertation, we use the functoriality differently to construct an invariant of closed surface generically immersed in a 4-manifold. The model for our construction is the Turaev-Viro construction of an invariant for a closed n -manifold with an infinite cyclic covering. The Turaev-Viro construction is based on an arbitrary n -TQFT and gives a module over the Laurent polynomial ring. See [3].

The new invariant is a bi-graded module over the Laurent polynomial ring $\mathbb{Q}[t, t^{-1}]$, where \mathbb{Q} is the field of rationals. More precisely, let $M = S^3 \times S^1$ and F be a closed surface generically immersed in M , we assign a module to the pair (M, F) using Khovanov homology and prove that it is invariant up to ambient isotopy.

Besides, we extend Khovanov homology to two new categories. The first category consists of oriented links as objects and morphisms are oriented immersed link cobordisms considered up to ambient isotopy. The second category has framed links as objects and morphisms are like in the first category besides that the cobordisms are not oriented and maybe even non-orientable. We proved that Khovanov homology is a ¹projective functor on both categories and the projective functoriality is used to define two versions of the generically immersed surface invariant as mentioned earlier.

Moreover, since $S^3 \times S^1$ can be obtained from S^4 by a surgery along a standardly embedded S^2 , the above construction can also be applied to generically immersed surfaces transversal to the standardly embedded 2-sphere in S^4 considered up to ambient isotopy.

This paper is organized as follows. In section 2, a definition of the Khovanov homology is outlined. In section 3, we generalize the link cobordisms and extend the projective functoriality of Khovanov homology to the generalized cobordisms. In section 4, a version of framed Khovanov homology is

¹A projective functor $F : \mathcal{C} \rightarrow \mathcal{D}$ is a functor $\mathcal{C} \rightarrow \mathcal{D}'$ where \mathcal{D}' is category with the same objects as \mathcal{D} and in which morphisms are morphisms in \mathcal{D} considered up to multiplication by ± 1

defined. In section 5, we construct the invariant of closed surface generically immersed in $S^3 \times S^1$ and its invariance considered up to *ambient isotopy* is proved. In section 6, various examples are studied. In section 7, we apply the construction to the generically immersed surface transversal to the standardly embedded S^2 in S^4 .

Chapter 2

Khovanov Homology

2.1 Khovanov Chain Complex

Given a link diagram D , a *marker* at each crossing is a bar specifying a pair of vertical angles at the crossing to be joined under smoothing of the crossing. See Figure 2.1.



Figure 2.1: Smoothings of a crossing according to markers

A Kauffman *state* s of D is a distribution of *markers* at all crossings. There are two types of *markers* for each crossing: positive marker \times and negative marker \times . For each state s , define $\sigma(s)$ as the difference of number

of positive markers and negative markers.

$$\sigma_+(s) = \#(\text{positive crossings}), \quad \sigma_-(s) = \#(\text{negative crossings}),$$

$$\sigma(s) = \sigma_+(s) - \sigma_-(s).$$

Let D_s be the result of resolution according to s and $|s|$ be the number of components of a smoothing along s . An *enhanced state* S of D is a Kauffman state s of D with an assignment of either $+$ or $-$ to each component of D_s . For an enhanced state S ,

$$\tau(S) = \tau_+(S) - \tau_-(S),$$

where $\tau_+(S)$ is the number of components in D_s with $+$, and $\tau_-(S)$ is the number of components with $-$. For an oriented diagram, each crossing is either positive, like $\nearrow \searrow$, or negative, like $\nwarrow \nearrow$. The *writhe number* of D is defined as the number of positive crossings minus the number of negative crossings. Denote it by $w(D)$. The bigrading (i, j) of the enhanced state S is defined as follows:

$$i(S) = \frac{w(D) - \sigma(S)}{2}, \quad j(S) = i(S) + w(D) + \tau(S).$$

Definition 2.1.1. *The (i, j) -th Khovanov chain complex $CKh^{i,j}(D)$ is a free abelian group generated by the enhanced states S of D with $i(S) = i$ and*

$$j(S) = j.$$

To define the differential of the Khovanov chain complex, we need an auxiliary structure. Fix an arbitrary ordering for all crossings of the diagram D . This ordering induces an ordering of negative markers in each state.

Definition 2.1.2. *Let S and T be two states, the **incidence number** of S and T , denote it by $[S : T]$ is a function satisfying following two conditions:*

1. $[S : T] = 0$ unless the markers of S and T differ at only one crossing and at this crossing the marker of S is positive and that of T is negative.
2. if S and T differs only at the k -th crossing, and if the number of negative marker after the k -th crossing is n , then $[S : T] = (-1)^n$.

For an enhanced state S , define a map d by

$$d(S) = \sum_T [S : T]T.$$

It has the following properties:

1. d is a homomorphism from $CKh^{i,j}(D)$ to $CKh^{i+1,j}(D)$
2. $d^2 = 0$

This d is the differential for the Khovanov chain complex, which gives rise to Khovanov homology.

Khovanov homology is proved to be invariant of Reidemeister moves and hence under isotopy by Khovanov [6].

2.2 Link Cobordisms and Movie Moves

Definition 2.2.1. A *link cobordism* between two links $L_0 \subset \mathbb{R}^3 \times \{0\}$ and $L_1 \subset \mathbb{R}^3 \times \{1\}$ is a compact surface F embedded in $\mathbb{R}^3 \times [0, 1]$ with boundary $\partial F = L_0 \cup L_1$. If F is oriented, then equip L_0 with the orientation induced from F , and L_1 with the orientation opposite to the one induced from F . With such orientation, F is called an **oriented link cobordism** between oriented links L_0 and L_1 .

Notice that there is a natural projection from F to $[0, 1]$. The preimage of its regular value t is a link $L_t = \mathbb{R}^3 \times \{t\} \cap F$.

We call an oriented link cobordism **generic** if the projection restricted to F is a Morse function with distinct critical points.

The intersections of a generic oriented link cobordism with hyperplanes of constant $t \in [0, 1]$ are embedded links except for a finite set of values. At these values, the intersection L_t has a single non-degenerate isolated double point corresponding to the critical point of the Morse function. Locally, the double point looks like \times at some time t .

A generic oriented link cobordism can be represented by a surface diagram in \mathbb{R}^3 . It is directly analogous to the two-dimensional link diagram. Such a diagram is the image of the oriented link cobordism under a projection to $\mathbb{R}^2 \times [0, 1]$ which preserves the last coordinate of the projection to $[0, 1]$. By an arbitrarily small perturbation, the projection can be made generic in the sense that the only singular points in the interior of the surface diagram are

double points, Whitney umbrella points and triple points. Whitney umbrellas occur as the (isolated) boundary points of the double point set in the interior of $\mathbb{R}^2 \times [0, 1]$. In order to recover the cobordism considered up to ambient isotopy, one needs to decorate the double points in the projection to distinguish the over crossing and under crossing, like \times .

We use *movie representation* to describe the oriented link cobordism similarly as in [4], and we consider oriented cobordisms up to *ambient isotopy* fixed on the boundary.

Definition 2.2.2. *Two oriented embedded surfaces F_1 and F_2 in a 4-manifold M are **ambient isotopic** if there is a family of diffeomorphisms*

$$H : M \times [0, 1] \longrightarrow M$$

such that $H(x, 0) = x$, and $H(F_1, 1) = F_2$.

Definition 2.2.3. *A **movie** of a generic oriented link cobordism with a given surface diagram is the intersection of the diagram with planes $\mathbb{R}^2 \times \{t\}$, regarded as a function of t . The intersection for a fixed t is called a **still**. The t for which the intersection is not a link diagram are called **critical levels**.*

Notice that the restriction of the movie to a small interval of time around a critical level shows a link diagram which undergoes either a Reidemeister move or a Morse modification. The Reidemeister moves occur at levels where

the double point set has a boundary point or a local maximum or minimum or triple points. More precisely, a boundary point corresponds to the first Reidemeister move, a local minimum or local maximum corresponds to the second Reidemeister move and the triple point corresponds to the third Reidemeister move. The Morse modifications occur at smooth points of the surface diagram which are local minimum, local maximum or saddle points of the projection function. Between two critical levels the diagram undergoes a planar isotopy.

Definition 2.2.4. *Reidemeister moves and Morse modifications will be called **local moves**. Each such move is localized in a small disc, called a **changing disc**.*

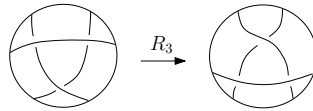


Figure 2.2: Third Reidemeister move in changing discs

Carter and Saito [11] found a complete set of moves analogous to Reidemeister moves for classic links, called *movie moves*. We borrowed movie move pictures from Clark, Morrison and Walker [2] and Carter and Saito [11] in Figure 2.3. Movie Move 1 - 10 are moves from the shown movie to the standard product of the first still and interval, which are omitted in the picture. Movie Move 11-15 are moves from one side to the other. And they proved that any two movies of ambient isotopic oriented link cobordisms can

be related by a sequence of movie moves and interchanges of distant critical points.

2.3 Two Categories and Khovanov Homology

Let \mathcal{C}'_o be a category whose objects are oriented links in general position such that their projections along z -axis are generic and morphisms are link cobordisms. Let \mathcal{C}'_d be a category whose objects are link diagrams and morphisms are movies. From the discussion above, we can see that there is a functor $F' : \mathcal{C}'_o \rightarrow \mathcal{C}'_d$. In fact, F' maps the oriented links to their projections along z -axis and maps the link cobordisms to movies. Moreover, let \mathcal{C}_o be the category whose objects are the same as in \mathcal{C}'_o and morphisms are morphisms in \mathcal{C}'_o considered up to ambient isotopy fixed on the boundary, and \mathcal{C}_d be the category whose objects are the same in \mathcal{C}'_d and morphisms are in \mathcal{C}'_d modulo movie moves, then F' induces a functor $F : \mathcal{C}_o \rightarrow \mathcal{C}_d$.

In the Khovanov construction, all the local moves induce chain maps on Khovanov chain complex. Hence any oriented link cobordism induces a chain map as a composition of local moves on Khovanov chain complex. In other words, let D_0 and D_1 be links diagrams of oriented links L_0 and L_1 and $F \subset \mathbb{R}^3 \times [0, 1]$ be a link cobordism with $F \cap \mathbb{R}^3 \times \{k\} = L_k \times \{k\}$ for $k = 0, 1$, and $\chi(F)$ be the Euler characteristic of the cobordism F , then F

induces a homomorphism

$$Kh^{i,j}(D_0) \longrightarrow Kh^{i,j+\chi(F)}(D_1).$$

Moreover, it is proved by Jacobsson [4] and Bar-Natan [1] that up to sign, movie moves 1-10 induce identity maps on Khovanov homology, and the two sides in Movie Move 11-15 induce the same map on Khovanov homology as well. Thus Khovanov homology is a projective functor $Kh : \mathcal{C}_d \longrightarrow \mathcal{V}$, where \mathcal{V} is the category of graded abelian groups. Moreover, the following diagram shows that Khovanov homology is a projective functor from \mathcal{C}_o to \mathcal{V} .

$$\begin{array}{ccccc}
 \mathcal{C}'_d & \xrightarrow{\quad} & \mathcal{C}_d & \xrightarrow{Kh} & \mathcal{V} \\
 \uparrow F' & & \uparrow F & \nearrow Kh' = Kh \circ F & \\
 \mathcal{C}'_o & \xrightarrow{\quad} & \mathcal{C}_o & &
 \end{array}$$

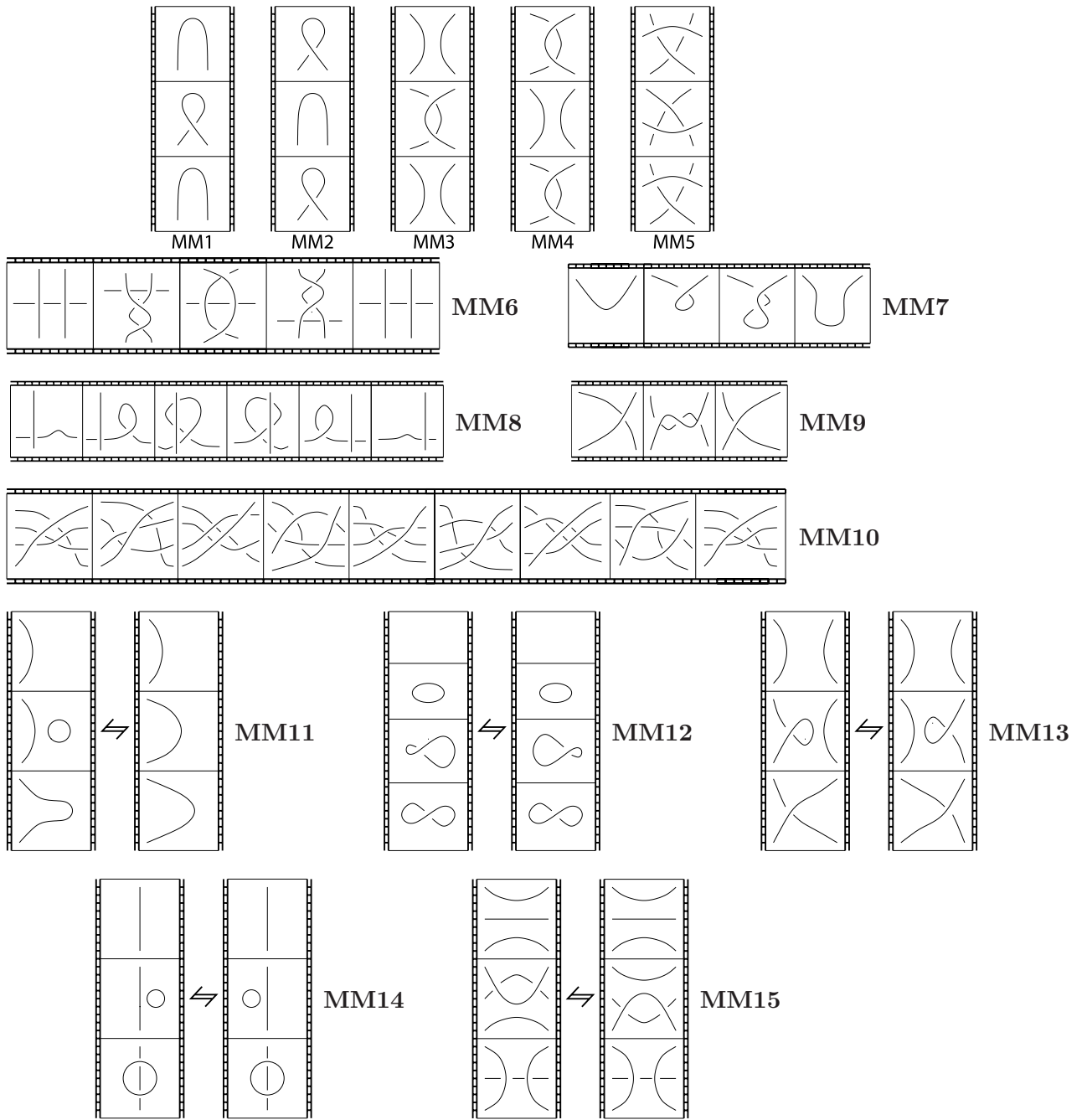


Figure 2.3: Carter and Saito's movie moves.

Chapter 3

Immersed Link Cobordisms and Khovanov Homology

3.1 Immersed Link Cobordisms

If we replace “embedded” by “immersed” in the definition of (oriented) link cobordism F in Definition 2.2.1, then F is called an *(oriented) immersed link cobordism*.

The immersed link cobordism is a generalization of the link cobordism. The main difference between them is that the immersed one also contains self-intersection points.

Definition 3.1.1. *An immersed link cobordism is **generic** if it has only transversal self-intersections.*

The intersections of a generic immersed link cobordism with hyperplanes

of constant $t \in [0, 1]$ are almost the same as the embedded case except that at a finite set of t it has one more types of single isolated double points, which corresponds to the transversal self-intersection of the surface. Locally it looks like \times at some t , which is exactly the same as the saddle point in the embedded case. They can be distinguished, however, by movies as we will see in the following.

A generic immersed link cobordism also has a 3-dimensional surface diagram and movie representation as described in Section 2.2. Local moves are Reidemeister moves and Morse modifications together with some extra move which is responsible for the self-intersection of the surface. We call it a crossing change move whose movie picture near the self-intersection looks like $\times \rightarrow \times \rightarrow \times$, which is in contrast to the double point corresponding to the saddle point whose local movie is like $\cup \rightarrow \times \rightarrow \cap$. Both types of double points lie in the interior of the set of double points in the surface diagram, thus the self-intersection of the surface would only interact with the second and third Reidemeister moves. Hence, the immersed link cobordism can be decomposed as Reidemeister moves and Morse modifications together with the crossing change move $\times \rightarrow \times \rightarrow \times$.

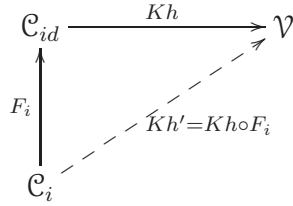
By replacing “embedded” with “immersed” in the definition of ambient isotopy in Section 2.2, we extend the notion of ambient isotopy to immersed surfaces. Again, we consider immersed cobordisms up to ambient isotopy fixed on the boundary.

For immersed link cobordisms, it is natural to ask the analogue of Movie

Moves as in Section 2.2. Certainly all the 15 types of Movie Moves as in Figure 2.3 are needed, while it is not sufficient since the self-intersection of the surface is involved. Since the double points corresponding to the self-intersections only interact with second and third Reidemeister moves as mentioned earlier, it suffices to have two extra movie moves as depicted in Figure 3.1. Thus, two immersed cobordisms are ambient isotopic if and only if they differ by a sequence of old and new movie moves together with an interchange of distant critical points.

3.2 Extend Khovanov Homology to a New Category

Let \mathcal{C}_i be a category whose objects are the same as in \mathcal{C}_o , the category of oriented links, and morphisms are oriented immersed link cobordisms considered up to ambient isotopy fixed on the boundary. Similarly as discussed in Section 2.3, we have a category of link diagrams corresponding to this category, denote by \mathcal{C}_{id} , which is almost the same as \mathcal{C}_d , the category of oriented link diagrams, except it includes extra morphisms which are movies with self-intersections modulo old and new movie moves. Hence there is a functor $F_i : \mathcal{C}_i \rightarrow \mathcal{C}_{id}$ which maps links to their generic projection and immersed link cobordisms to movies. To extend the Khovanov homology over \mathcal{C}_i , it suffices to extend it over \mathcal{C}_{id} .



Since the only extra movies are those involving double point corresponding to the transversal self-intersection of the surface as we have seen in Section 3.1, it suffices to show that the induced maps of two sides of the extra movie moves as in Figure 3.1 differ at most by a sign on Khovanov homology.

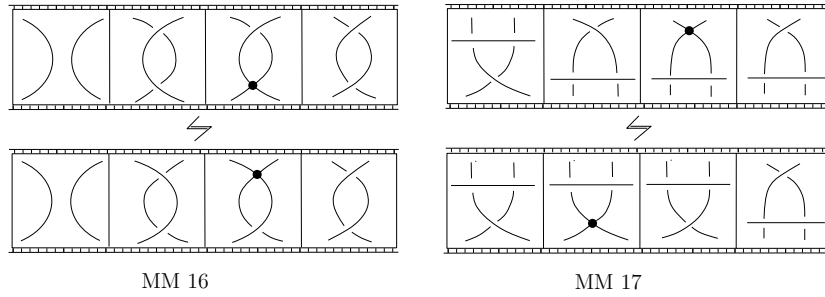
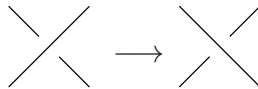


Figure 3.1: Extra Movie Moves. The solid dots are the transversal self-intersection points.

Notice that in the extra moves, there is a local crossing change move which doesn't appear in the original Khovanov construction.



We define the crossing change map c_1 in the following.

$$c_1 : CKh^{i,j}(\nearrow \searrow) \longrightarrow CKh^{i,j-2}(\nearrow \searrow),$$

where $CKh^{i,j}(\ast)$ is the Khovanov chain complex.

$$c_1(\times) = \times,$$

$$c_1(\overline{\times}) = 0.$$

To see how the grading change, we recall the definition of the bigrading (i, j) of Khovanov chain complex in terms of Kauffman *enhanced states* as defined in Section 2.3. By definition, c_1 preserves τ , while changing w and σ accordingly. Eventually, c_1 preserves i grading, while decreasing j grading by 2.

It is easy to check the following diagram commutes:

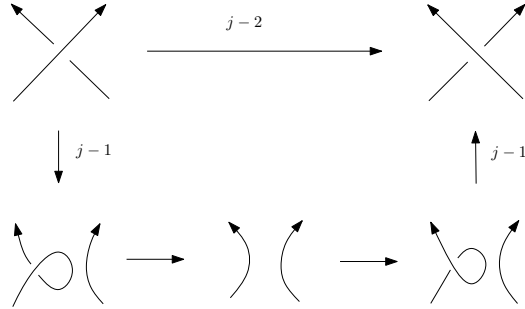
$$\begin{array}{ccc} CKh^{i,j}(\nearrow \searrow) & \xrightarrow{c_1} & CKh^{i,j-2}(\nearrow \searrow) \\ \downarrow d & & \downarrow d \\ CKh^{i-1,j}(\nearrow \searrow) & \xrightarrow{c_1} & CKh^{i-1,j-2}(\nearrow \searrow) \end{array}$$

where d is the differential of Khovanov chain complex.

Corollary 3.2.1. $c_1 : CKh^{i,j}(\nearrow \searrow) \longrightarrow CKh^{i,j-2}(\nearrow \searrow)$ is a chain map.

Moreover, this crossing change homomorphism is equivalent to the com-

position of Reidemeister moves and Morse modifications as shown below:



We call the double point corresponding to c_1 the Type 1 double point.

Similarly, we define

$$c_2 : Kh^{i,j}(\nearrow \searrow) \longrightarrow Kh^{i+2,j+4}(\nearrow \searrow)$$

$$c_2(\times) = \times$$

$$c_2(\bowtie) = 0$$

The grading is changed differently due to the change of writhe number, and interestingly it doesn't have similar decomposition as the one above due to orientation reason.

We call the double point corresponding to c_2 the Type 2 double point. Similarly, it is easy to check that c_2 commutes with the differential of Khovanov chain complex.

Corollary 3.2.2. $c_2 : Kh^{i,j}(\nearrow \searrow) \longrightarrow Kh^{i+2,j+4}(\nearrow \searrow)$ is a chain map.

With the crossing change homomorphism above, we can define the map

induced by cobordisms with both two types of double points, which is just the composition of maps induced by local moves together with the crossing change maps.

Let D_0 and D_1 be links diagrams of oriented links L_0 and L_1 and $F \subset \mathbb{R}^3 \times [0, 1]$ be an immersed link cobordism with $F \cap \mathbb{R}^3 \times \{k\} = L_k \times \{k\}$ for $k = 0, 1$, d_i be the number double points of Type i where $i = 1, 2$ and $\chi(F)$ be the Euler characteristic of the cobordism F , then F induces a homomorphism

$$Kh^{i,j}(D_0) \longrightarrow Kh^{i+2d_2, j-2d_1+4d_2+\chi(F)}(D_1).$$

Direct calculation shows that the homomorphisms induced by the two sides of extra movie moves in Figure 3.1 differ only by a sign. The detailed calculation can be found in Appendix A.

Theorem 3.2.1. *Khovanov homology is a projective functor from the category \mathcal{C}_i to the category of graded abelian groups.*

We call this extended version *immersed Khovanvo homology*.

Remark. Notice that the bigrading of Khovanov chain complex depends on the orientation of the link diagram. If we take the total group $C = \oplus CKh^{i,j}(D)$, then the differential on Khovanov chain complex defines a differential on C , then neither C nor the differential on C depends on the orientation of the diagram. Moreover, the two versions of the crossing change maps on this total group are the same. In the next section, we will see that without orientation, the crossing change map can be defined as a composition

of two simple maps, and there is only one version of such map.

Chapter 4

Framed Khovanov Homology

4.1 Framed links and diagrams

A **framed** link is a closed 1-dimensional smooth submanifold in \mathbb{R}^3 with a *framing*, which is a non-vanishing normal vector field. Intuitively, a framed link can be considered as a ribbon that can be obtained by pushing the link along the normal vector field. See Figure 4.1. We consider framings up to isotopy. A link diagram defines a class of isotopic framings whose vectors are projected to non-zero vectors. These framings are called *blackboard framing*. We consider all possible framings, not only blackboard ones.

We can draw a framed link diagram as in Figure 4.1, but this would be superfluous and cumbersome. All we need is the information that would allow to recover the framing of the link from the diagram up to isotopy. One way to achieve this is explained below.

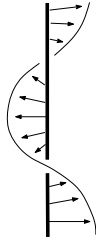


Figure 4.1: Local picture for a framing

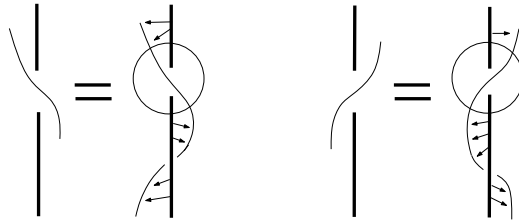


Figure 4.2: Decoration framings

Instead of drawing the whole ribbon as in Figure 4.1, we draw only a part of the picture where the curve obtained by pushing the link along the normal vector field is shown only near points where it is above the link. See Figure 4.2. Since we consider framings up to isotopy, this drawing or decoration contains sufficient information to recover the framing of the whole link. In particular, if the framing is blackboard, then no decoration appears. See an example of framed link diagram in Figure 4.3.

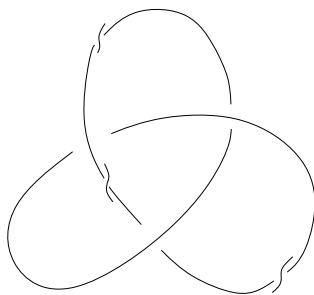


Figure 4.3: A framed trefoil

4.2 Normal Euler Number

Let \mathcal{N} be the normal bundle of the immersed link cobordism in $S^3 \times [0, 1]$. A **normal Euler number** of \mathcal{N} , defined by Whitney in [13], is the obstruction for extending the framing of the boundary links to a nowhere zero section of \mathcal{N} .

Geometrically this number can be interpreted in the following.



Let s_0 be the zero section of \mathcal{N} , and s be another section of \mathcal{N} such that it extends the framings on the boundary links to the whole cobordism. At each zero x of s , the local orientation of s_0 induces a local orientation of s , both of which together define a local orientation in the neighborhood of x . It does not depend on the choice of local orientation of s_0 because if s_0 changes orientation, the orientation of s is also changed. Thus the induced the local orientation near x does not change.

On the other hand, since $S^3 \times [0, 1]$ is oriented, it also defines an orientation in a neighborhood of x .

Definition 4.2.1. *A local intersection number of s and s_0 at x is a number of ± 1 . It is $+1$ if the local orientation induced by the ambient manifold is the same as the one induced by s and s_0 , -1 otherwise.*

The normal Euler number of \mathcal{N} is just the sum of local intersection numbers of s and s_0 at all zeros. Thus, this number is defined even if the underlying link cobordism is non-orientable and it is always an integer.

4.3 Framed Khovanov homology

The framed Khovanov homology is first defined by Viro [14]. In that definition, only blackboard framing is considered. In our setup, the following additional characteristic is needed. Denote by $fr(D)$ the difference of the number of positive twists t_+ , like  , and the number of negative twists t_- , like  , in all component:

$$fr(D) = \#t_+(D) - \#t_-(D),$$

where D is the link diagram. For example, for the framed trefoil in Figure 4.3, $fr = -1$.

We consider framed links under framing preserving isotopy. The analogue of Reidemeister moves for oriented links are obtained in the following. Since the original first Reidemeister move doesn't preserve $fr(D)$, we modify it as in Figure 4.4. The original second and third Reidemeister moves are used

without change since they don't change $fr(D)$. Two extra twist moves as depicted in Figure 4.5 and Figure 4.6 are included. Then two framed links are isotopic if and only if they differ by a sequence of these modified Reidemeister moves and twist moves.

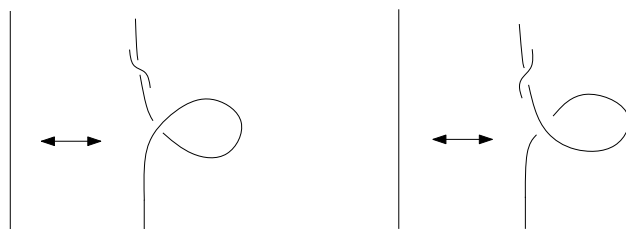


Figure 4.4: The first framed Reidemeister moves

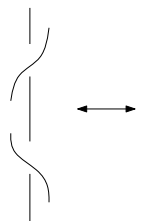


Figure 4.5: Twist annihilation move

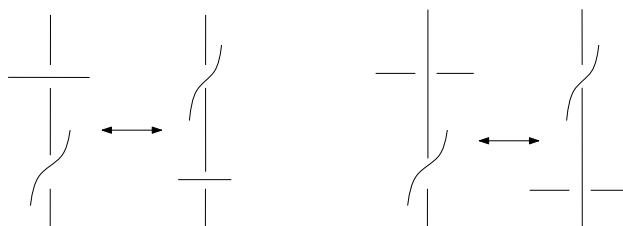


Figure 4.6: Twist penetration move

We use the same notations as in [14] to define the chain complex of the

framed Khovanov homology. Let s be a Kauffman state of D as defined in Section 2.3.

$$\sigma_+(s) = \#(\text{X}), \quad \sigma_-(s) = \#(\text{Y}),$$

$$\sigma(s) = \sigma_+(s) - \sigma_-(s).$$

$|s|$ is the number of components of a smoothing along s . With the Kauffman skein relation

$$\langle \text{X} \rangle = A \langle \text{Z} \rangle + A^{-1} \langle \text{W} \rangle,$$

it is easy to show that the Kauffman bracket

$$\langle D \rangle = \sum_s (-A)^{3fr(D)} A^{\sigma(s)} (-A^2 - A^{-2})^{|s|}$$

is invariant up to framing preserving isotopy.

Let S be an enhanced state of D as defined in Section 2.3,

$$\tau(S) = \tau_+(S) - \tau_-(S),$$

we define a new bigrading (p, q) for an enhanced state S

$$p(S) = \tau(S) - fr(D), \quad q(S) = \sigma(S) - 2\tau(S) + 3fr(D).$$

The framed Khovanov chain complex $C^{p,q}(D)$ is a bi-graded \mathbb{Z} -module gen-

erated by the enhanced states, the differential

$$d : C^{p,q}(D) \longrightarrow C^{p-1,q}(D)$$

is defined the same as in Khovanov homology. It is well-defined up to an overall grading shift due to $fr(D)$. In other words, (p, q) is well-defined up to a k multiple of $(1, -3)$ where $k \in \mathbb{Z}$. We denote the homology of $C^{p,q}(D)$ by $Kh_{fr}^{p,q}(D)$. If we fix a framing and an orientation on a link, there is a one-to-one correspondence between Khovanov chain complex and framed Khovanov chain complex. More precisely, recall that the bi-grading (i, j) of the Khovanov chain complex is defined as

$$i(S) = \frac{w(D) - \sigma(S)}{2}, \quad j(S) = i(S) + w(D) + \tau(S).$$

Then if

$$p(S) = j(S) - i(S) - w(D) - fr(D), \quad q(S) = -2j(S) + 3w(D) + 3fr(D),$$

we have

$$C^{p,q}(D) = CKh^{i,j}(D).$$

In other words, the total group $\bigoplus_{p,q} C^{p,q}(D) = \bigoplus_{i,j} CKh^{i,j}(D)$. Thus we can use the same chain map for all Reidemeister moves as defined in the original Khovanov construction to define the corresponding maps in the framed

version. For the two extra framed moves: twist annihilation and penetration moves, the induced chain maps are just identity since neither the enhanced state nor the grading are changed under these moves. It is easy to check that the framed Khovanov homology is invariant of all framed Reidemeister moves and extra framing preserving moves.

Corollary 4.3.1. *Framed Khovanov homology is invariant of framed links consider up to framing preserving isotopy.*

Next, we consider chain maps on framed Khovanov chain complex induced by the immersed link cobordisms.

First of all, we consider the special cobordism $F = L \times [0, 1]$, where L is a link. Let D_0, D_1 be two framed link diagrams which are identical link diagrams of L with different framings. Let $e \in \mathbb{Z}$ be the normal Euler number of the normal bundle of F as described in Section 4.2. The induced chain map on the framed Khovanov chain complex changes nothing but the bi-grading. In other words, F induces a homomorphism on the framed Khovanov homology

$$Kh_{fr}^{p,q}(D_0) \longrightarrow Kh_{fr}^{p-e,q+3e}(D_1).$$

Second, we consider cobordisms consisting of Morse modifications (surgeries).

There are three kinds of surgeries: 0, 1, 2-surgeries. The induced maps on chain level use the corresponding maps defined in the original Khovanov chain complex.

0(2)-surgery creates(annihilates) framed circles as in Figure 4.7. The framing is changed when necessary in the middle step. Thus the 0, 2-surgeries on framed Khovanov homology is defined as a composition of the framing change map and the corresponding surgery map in the original Khovanov homology.

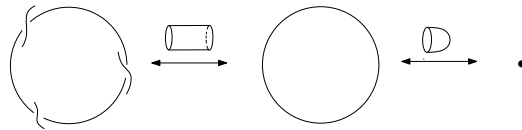


Figure 4.7: 0,2-surgeries.

1-surgery merges two framed arcs. Notice that there are two types of 1-surgeries:

1. The framing on the two arcs are compatible.

We can just merge them as in Figure 4.8.

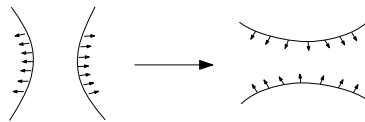


Figure 4.8: 1-surgery along two compatible framed arcs

2. The framings on the two arcs are not compatible.

We cannot just merge them as in the first case. However, we can always add some twists to one of the arcs so that the framings are compatible and then merge them as in the first type. $fr(D)$ is unchanged. See Figure 4.9.

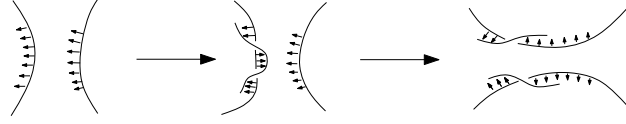
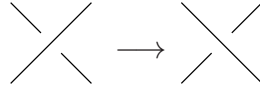


Figure 4.9: 1-surgery along two non-compatible framed arcs

Third, we consider a cobordism with double points corresponding to self-intersections of the surface. As seen in Section 3.1, we need a crossing change map for



We use the Kauffman skein relation below to define this map.

$$\langle \times \rangle = A \langle \rangle + A^{-1} \langle \smile \rangle$$

This relation also gives a short exact sequence of complexes:

$$0 \longrightarrow C^{p,q}(\smile) \xrightarrow{\alpha} C^{p,q-1}(\times) \xrightarrow{\beta} C^{p,q-2}(\rangle) \longrightarrow 0$$

where α is the inclusion and β is the projection. The composition

$$C^{p,q}(\times) \xrightarrow{\beta} C^{p,q-1}(\rangle) \xrightarrow{\alpha} C^{p,q-2}(\times)$$

defines a chain map $c = \alpha \circ \beta : CKh_{fr}^{p,q}(\times) \longrightarrow CKh_{fr}^{p,q-2}(\times)$, then c

induces a homomorphism on the framed Khovanov homology.

$$c : Kh_{fr}^{p,q}(\times) \longrightarrow Kh_{fr}^{p,q-2}(\times)$$

Notice that there is only one type of such map in contrast to the two types in the oriented case, and the following diagram commutes up to a grading shift.

$$\begin{array}{ccc}
 \begin{array}{c} \diagup \quad \diagdown \\ \diagdown \quad \diagup \end{array} & \xrightarrow{q-2} & \begin{array}{c} \diagdown \quad \diagup \\ \diagup \quad \diagdown \end{array} \\
 \downarrow p-1, q+2 & & \uparrow p-1, q+2 \\
 \begin{array}{c} \text{loop} \left(\longrightarrow \right) \left(\longrightarrow \right) \end{array} & & \begin{array}{c} \left(\longrightarrow \right) \left(\longrightarrow \right) \text{loop} \end{array}
 \end{array}$$

With the homomorphism above we can similarly define the induced map of an immersed link cobordism on framed Khovanov homology. Let D_0 and D_1 be link diagrams of two framed links L_0 and L_1 , $F \subset \mathbb{R}^3 \times [0, 1]$ be an immersed compact surface with $F \cap \mathbb{R}^3 \times \{k\} = L_k \times \{k\}$ for $k = 0, 1$, e be the normal Euler number of the normal bundle of F , and d be the number of transversal self-intersection points. Then the cobordism F induces an homomorphism

$$Kh_{fr}^{p,q}(D_0) \longrightarrow Kh_{fr}^{p+\chi(F)-e, q-2\chi(F)+3e-2d}(D_1).$$

4.4 Categories of framed links and their diagrams

Let \mathcal{C}'_{fr} be a category whose objects are framed links that are in general position such that their projection along z -axis are generic and morphisms are immersed link cobordisms, \mathcal{C}'_{frd} be the category of framed link diagrams as described in Section 4.1 and morphisms are movies of immersed link cobordisms. Let \mathcal{C}_{fr} be the category whose objects are the same as in \mathcal{C}'_{fr} and morphisms are the morphisms in \mathcal{C}'_{fr} considered up ambient isotopy fixed on the boundary, \mathcal{C}_{frd} be the category with the same objects in \mathcal{C}'_{frd} and the same morphisms in \mathcal{C}'_{frd} modulo movie moves in Section 3.2. Then there is functor $Fr' : \mathcal{C}'_{fr} \longrightarrow \mathcal{C}'_{frd}$, which maps the framed links in general position to its generic projection along z -axis and immersed link cobordisms to movies as described in Section 3.2. Moreover, since the morphisms in \mathcal{C}'_{fr} and \mathcal{C}'_{frd} are immersed link cobordisms and their corresponding movie moves, Fr' induces a projective functor $Fr : \mathcal{C}_{fr} \longrightarrow \mathcal{C}_{frd}$. Moreover, we have the following result.

Corollary 4.4.1. *The framed Khovanov homology is a projective functor from category \mathcal{C}_{fr} to category \mathcal{V} .*

Proof. By the projective functoriality of the immersed Khovanov homology, the framed Khovanov homology is also a projective functor from \mathcal{C}_{frd} to \mathcal{V} in Section 4.3.

On the other hand, we have the following commutative diagram.

$$\begin{array}{ccccc}
 \mathcal{C}'_{frd} & \xrightarrow{\quad} & \mathcal{C}_{frd} & \xrightarrow{Kh_{fr}} & \mathcal{V} \\
 \uparrow Fr' & & \uparrow Fr & \nearrow Kh'_{fr} = Kh_{fr} \circ Fr & \\
 \mathcal{C}'_{fr} & \xrightarrow{\quad} & \mathcal{C}_{fr} & &
 \end{array}$$

Hence the composition $Kh_{fr} \circ Fr$ is a projective functor from \mathcal{C}_{fr} to \mathcal{V} . \square

Remark. The difference between the framed Khovanov homology and the original Khovanov homology is not just in their gradings. For example, in the original version, we cannot do 1-surgery along two arcs with the same orientation, like $\int \int$, while in the framed version, we can always merge two arcs (by adding twists if necessary). This difference will be further illustrated in examples in Section 6.

Chapter 5

The Construction of the New Invariant

5.1 The construction

Let F be a generically immersed 2-manifold in $S^3 \times S^1$, L be the transversal intersection

$$L = S^3 \times \{1\} \cap F.$$

Let \tilde{F} be the preimage of F under the infinite cyclic covering map

$$S^3 \times \mathbb{R} \longrightarrow S^3 \times S^1 : (x, y) \longrightarrow (x, e^{2i\pi y}),$$

$$L_n = \tilde{F} \cap (S^3 \times \{n\}) \subset S^3 \times \mathbb{R},$$

and

$$F_n = \tilde{F} \cap (S^3 \times [n, n+1]).$$

By the functoriality of Khovanov homology, the cobordism induces a linear map

$$Kh(F_n) : Kh^{i,j}(L) \longrightarrow Kh^{i,j+\chi(F_n)}(L),$$

where $\chi(F_n)$ is the Euler characteristic of F_n . For simplicity, we only consider the Khovanov homology with \mathbb{Q} coefficient and the functoriality is understood as projective functoriality and the equality on Khovanov homology holds up to sign.

Since Khovanov homology has finite rank, the following increasing sequences of kernels will stabilize.

$$\ker Kh(F_0) \subset \ker Kh(F_0 \cup F_1) \subset \cdots \subset Kh(L_0)$$

Let

$$V_s(L_0) := \bigcap_{j=1}^{\infty} \text{Im}(Kh(\cup_{n=-j}^{-1} F_n)) \cong Kh(L_0) / \ker(Kh(\cup_{n=0}^{\infty} F_n)).$$

$V_s(L_0)$ is also called the *stabilized image* of $Kh(L_0)$. If we denote the restriction of $Kh(F_0)$ on $V_s(L_0)$ by $Kh_s(F_0)$, it is not difficult to see that $V_s(L_0)$ is a $\mathbb{Q}[t, t^{-1}]$ -module with t acting by $Kh_s(F_0)$. We denote this module by $\mathcal{M}(F)$. Notice that t naturally has degree 0, since otherwise the stabilized image $V_s(L_0) = 0$.

Theorem 5.1.1 (Viro). $\mathcal{M}(F)$ does not depend on L_0 , and it is well-defined up to $\mathbb{Q}[t, t^{-1}]$ -module isomorphisms.

Proof. Let $s \in [0, 1]$ and $L' \equiv S^3 \times \{e^{2si\pi}\} \cap F$ be another transversal intersection away from L . We can similarly define

$$L'_n = F \cap (S^3 \times \{n + s\}) \subset S^3 \times \mathbb{R}$$

and

$$F'_n = F \cap (S^3 \times [n + s, n + s + 1]).$$

Let T be the deck transformation of the infinite cyclic cover of $S^3 \times S^1$. Define

$$E_k = \begin{cases} \cup_{0 \leq i \leq k-1} T^i(F_0) & k \in \mathbb{Z}^+ \\ \cup_{k \leq i \leq -1} T^i(F_0) & k \in \mathbb{Z}^- \end{cases},$$

and E'_k is defined similarly with F_0 replaced by F'_0 . Let W be the cobordism between L_0 and L'_0 , we will show that $Kh(W)$ maps $V_s(L_0)$ to $V_s(L'_0)$ in the following.

Let $x \in V_s(L_0)$ and $Kh(W)(x) = x'$, then by the definition of $V_s(L_0)$, there exists some $n > 0$ such that $x \in Kh(E_{-n})(Kh(T^{-n}(L_0)))$. Hence $x = Kh(E_{-n})(y)$ for some y . Let $Kh(T^{-n}(W))(y) = y'$, then

$$x' = Kh(W)x = Kh(W) \circ Kh(E_{-n})(y).$$

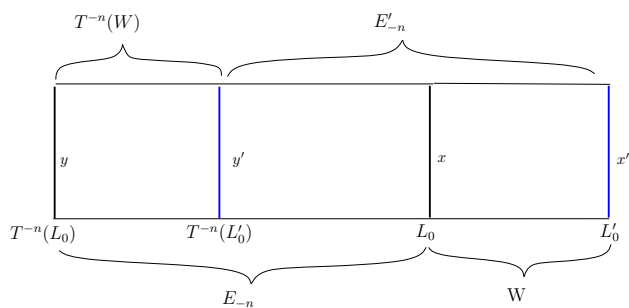


Figure 5.1: Composition of cobordisms

On the other hand, since

$$E_{-n} \cup W = T^{-n}(W) \cup E'_{-n},$$

by the functoriality of Khovanov homology,

$$Kh(E_{-n} \cup W) = Kh(W) \circ Kh(E_{-n}),$$

$$Kh(T^{-n}(W) \cup E'_{-n}) = Kh(E'_{-n}) \circ Kh(T^{-n}(W)).$$

Hence

$$\begin{aligned}
x' &= Kh(W)x \\
&= Kh(W) \circ Kh(E_{-n})(y) \\
&= Kh(E_{-n} \cup W)(y) \\
&= Kh(T^{-n}(W) \cup E'_{-n})(y) \\
&= Kh(E'_{-n}) \circ Kh(T^{-n}(W))(y) \\
&= Kh(E'_{-n})(y') \in V_s(L'_0)
\end{aligned}$$

See Figure 5.1.

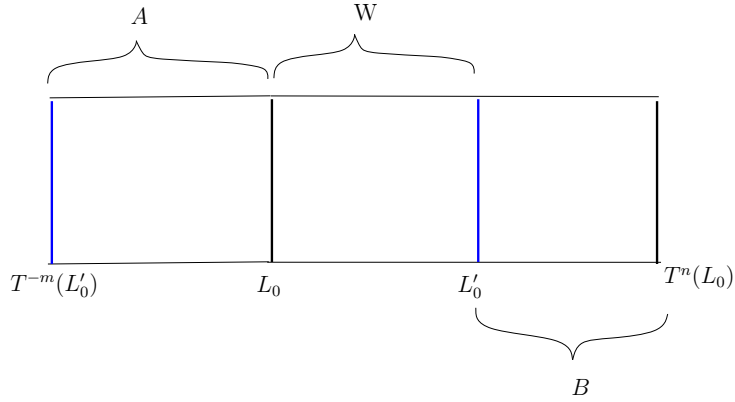


Figure 5.2: $Kh_s(W)$ is an isomorphism

Moreover, we will show that the restriction $Kh_s(W) : V_s(L_0) \longrightarrow V_s(L'_0)$ is an isomorphism.

Let $L'_0 \subset E_\infty$, then there exist integers m and n such that $Kh_s(A \cup W)$ and $Kh_s(W \cup B)$ are both isomorphisms by the definition of Kh_s . See Figure

5.2. By the functoriality of Khovanov homology again,

$$Kh_s(A \cup W) = Kh_s(W) \circ Kh_s(A),$$

$$Kh(W \cup B)_s = Kh(B)_s \circ Kh(W)_s,$$

thus $Kh(W)_s$ is an isomorphism.

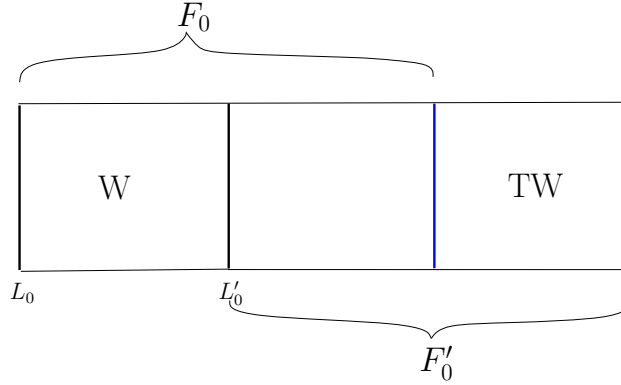


Figure 5.3: $Kh_s(F_0) \cong Kh_s(W)^{-1} \circ Kh_s(F_0') \circ Kh_s(W)$ in case (1)

What's more, we will prove that $\mathcal{M}(F)$ is well-defined up to $\mathbb{Q}[t, t^{-1}]$ -module isomorphisms.

Consider the following two cases:

(1) $W \subset F_0$, then

$$W \cup F_0' = F_0 \cup TW.$$

Since $Kh_s(W) = Kh_s(TW)$, the functoriality of Khovanov homology implies

$$Kh_s(F_0') \circ Kh_s(W) = Kh_s(TW) \circ Kh_s(F_0).$$

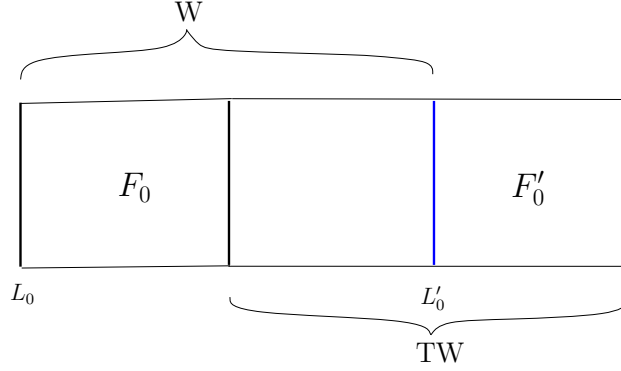


Figure 5.4: $Kh_s(F_0) \cong Kh_s(W)^{-1} \circ Kh_s(F'_0) \circ Kh_s(W)$ in case (2)

(2) $F_0 \subset W$, then

$$W \cup F'_0 = F_0 \cup TW.$$

Similarly, we have

$$Kh_s(F'_0) \circ Kh_s(W) = Kh_s(TW) \circ Kh_s(F_0).$$

see Figure 5.4. The proof is complete. \square

We will show see that $\mathcal{M}(F)$ is invariant of ambient isotopy in the next section.

5.2 An isotopy invariant

Theorem 5.2.1. *If F and F' are ambient isotopic surfaces generically immersed in $S^3 \times S^1$, then $\mathcal{M}(F) \cong \mathcal{M}(F')$ as $\mathbb{Q}[t, t^{-1}]$ -modules.*

Proof. We use the same notation F and F' to represent be the images of the corresponding immersions. Let $H : F \times [0, 1] \longrightarrow S^3 \times S^1$ be an ambient isotopy such that

$$H_0(x) \equiv H(x, 0) = x \quad \text{and} \quad H_1(F) \equiv H(F, 1) = F'.$$

By *Thom's isotopy extension theorem* [5], this isotopy can be extended to $S^3 \times S^1 \times [0, 1]$. We denote it by the same H .

Since $S^3 \times \mathbb{R} \times [0, 1]$ is simply connected, H can be lifted as \tilde{H} on its infinite cyclic cover $S^3 \times \mathbb{R} \times [0, 1]$.

$$\begin{array}{ccc} S^3 \times \mathbb{R} \times [0, 1] & \xrightarrow{\tilde{H}} & S^3 \times \mathbb{R} \\ \downarrow & & \downarrow \\ S^3 \times S^1 \times [0, 1] & \xrightarrow{H} & S^3 \times S^1. \end{array}$$

Denote the lifting of F and F' by \tilde{F} and \tilde{F}' respectively, let F_n and F'_n be the transversal intersections,

$$F_n = \tilde{F} \cap (S^3 \times [n, n + 1]) \quad \text{and} \quad F'_n = \tilde{F}' \cap (S^3 \times [n, n + 1]),$$

then \tilde{H}_1 is a self-diffeomorphism of $S^3 \times \mathbb{R}$ such that

$$\tilde{H}_1(\tilde{F}) = \tilde{F}'.$$

Let $L_0 = \tilde{F} \cap (S^3 \times \{0\})$ and $L'_0 = \tilde{F}' \cap (S^3 \times \{0\})$, then

$$\tilde{H}^{-1}(L'_0) = \tilde{H}^{-1}(\tilde{F}') \cap \tilde{H}^{-1}(S^3 \times \{0\}) = \tilde{F} \cap \tilde{H}^{-1}(S^3 \times \{0\})$$

defines a cobordism between L_0 and $\tilde{H}_1^{-1}(L'_0)$. See Figure 5.5.

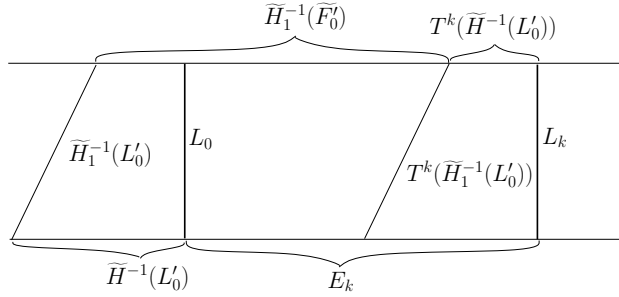


Figure 5.5: A cobordism induced by the isotopy of diffeomorphisms

Now we are in a very similar situation as in Theorem 5.1.1 except now we have $\tilde{H}_1^{-1}(L'_0)$ sitting inside a skewed copy of S^3 . In other words, the boundary of the cobordism $\partial(\tilde{H}^{-1}(L'_0))$ is not in $S^3 \times \{point\}$. Thus we cannot apply Khovanov homology to this cobordism. To apply the same argument, we need to modify the cobordism.

First, we choose a cobordism $\cup_{i=0}^{n+k} F_i \subset \tilde{F}$ such that the induced map on Khovanov homology is stabilized, i.e. the kernel is not increasing.

Second, we choose another stabilized cobordism $\cup_{i=m}^{m+k'} F'_i \subset \tilde{F}'$ with m, k' large enough so that the pull back $\tilde{H}_1^{-1}(\cup_{i=m}^{m+k'} F'_i)$ is away from $\cup_{i=0}^{n+k} F_i$.

Third, we choose another copy of the link L , say L_p so that $\tilde{H}_1^{-1}(\cup_{i=m}^{m+k'} F'_i)$ is between L_0 and L_p as depicted in Figure 5.6.

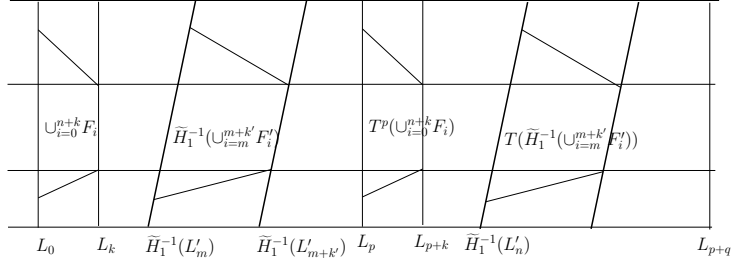


Figure 5.6: Pull back cobordism in \tilde{F}

Suppose L_p is far away from this pull back cobordism. We can use the isotopy H to construct a new ambient isotopy ϕ in a neighborhood of $\tilde{H}_1^{-1}(S^3 \times [m, m + k'])$. More precisely,

$$\phi : S^3 \times [k, p] \times [0, 1] \longrightarrow S^3 \times [k, p]$$

such that $\phi(x, i, t) = x, \phi(x, i, 0) = x$ if $i = k, p$ and

$$\phi(\tilde{H}_1^{-1}(S^3 \times [m, m + k']), 1) = S^3 \times [m, m + k'].$$

Under this isotopy, the pull back cobordism will be in the product space $S^3 \times [m, m + k']$ as depicted in Figure 5.7. Denote $\phi(\cdot, \cdot, 1)$ by ϕ_1 . There is a cobordism W connecting L_k and $\phi_1(\tilde{H}_1^{-1}(L'_m))$ as in Figure 5.7.

Moreover, we can do the same trick to extend the isotopy ϕ to the next product space $S^3 \times [p, p + q]$ for some large q , so that ϕ fixes L_p and L_{p+q} . Under this isotopy, we have a cobordism $W \cup \phi_1(\tilde{H}_1^{-1}(U_{i=m'}^{n-1} F'_i))$ connecting L_k and $\phi_1(\tilde{H}_1^{-1}(L'_n))$ in Figure 5.7.

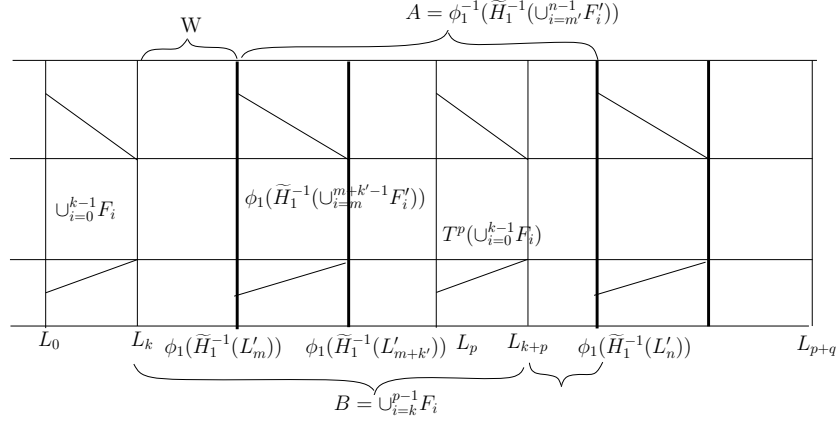


Figure 5.7: New cobordisms under ambient isotopy ϕ_t .

Now the same argument as in Theorem 5.1.1 shows that

$$Kh_s(A) \cong Kh_s(TW) \circ Kh_s(B) \circ Kh_s(W)^{-1},$$

where $A = \tilde{H}_1^{-1}(\cup_{i=m'}^{n-1} F'_i)$ and $B = \cup_{i=k}^{p-1} F_i$.

Since

$$Kh_s(A) \cong Kh_s(F'_0), \quad Kh_s(B) \cong Kh_s(F_0),$$

the theorem is proved. \square

Notice that the construction of $\mathcal{M}(F)$ and the proof of the Theorem 5.2.1 mainly uses the functoriality of Khovanov homology. Both will also work if we replace Khovanov homology with the framed version. We summarize the result in the following.

Corollary 5.2.1. *$\mathcal{M}(F)$ and $\mathcal{M}_{fr}(F)$ are invariants of generically closed*

immersed surfaces in $S^3 \times S^1$ considered up to ambient isotopy.

For the rest of the paper, we denote $\mathbb{Q}[t, t^{-1}]$ by R . $\mathcal{M}(F)$ and $\mathcal{M}_{fr}(F)$ are bi-graded R -modules. Since R is a Principle Ideal Domain, we can write every summand of each invariant as the direct sum of quotients of R . More precisely, let f_1, f_2, \dots, f_m be the invariant factors of the matrix of the stabilized Khovanov homology such that for all i ,

$$f_i | f_{i+1},$$

then by the *Structure theorem for finitely generated modules over a principal ideal domain*, we have the following isomorphism

$$\mathcal{M}^{i,j}(F) \cong R/f_1 \oplus \dots \oplus R/f_m.$$

\mathcal{M} can be replaced with \mathcal{M}_{fr} . In all the examples below, the invariant(s) will take this form.

Chapter 6

Examples

We have seen the construction of the surface invariant $\mathcal{M}(F)$ for a closed generically immersed surface F in $S^3 \times S^1$ in Chapter 5. The main idea is cutting the closed surface in the middle and applying Khovanov homology to the resulting cobordism which connects two identical links, and we have proved that the result doesn't depend on how we cut it. In this Chapter, we construct cobordisms which connect two identical links and apply various versions of Khovanov homology to compute the invariant \mathcal{M} of the "close-up" surfaces obtained by identifying two ends of the cobordisms. We compute examples of surfaces obtained by planer isotopies, Reidemeister moves or surgeries. The brief summary of figures and results are listed below.

1. Product surface $F = L \times [0, 1]$.

$$\mathcal{M}^{i,j}(\overline{F}) \cong Kh^{i,j}(L) \otimes \mathbb{Q} \cong (R/(t-1))^{rkKh^{i,j}(L)}.$$

See Subsection 6.1.1 for details.

- Two examples of Rotations: Trefoil knot and Knot(8,18).

Corollary 6.0.2. *Let $F_{tref} \equiv T \times [0, 1] /_{T \times \{0\} \sim \rho(T) \times \{1\}}$ as in Figure 6.1, where T is the trefoil knot, ρ is the rotation, then*

$$\mathcal{M}^{i,j}(F_{tref}) \cong Kh^{i,j}(T) \otimes \mathbb{Q}.$$

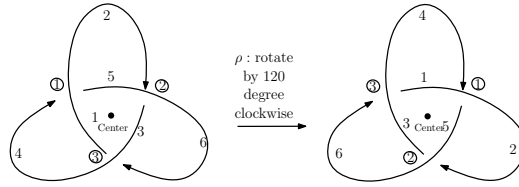


Figure 6.1: Rotate a trefoil knot clockwise by 120 degree

Corollary 6.0.3. *Let F_t be the surface obtained by rotating $Knot(8,18)$ clockwise 90 degree in Figure 6.2, then $\mathcal{M}^{i,j}(F_t)$ admits a nontrivial R action on $Kh^{i,j}(K)$ if the Betti number of $Kh^{i,j}(K)$ is larger than 1.*

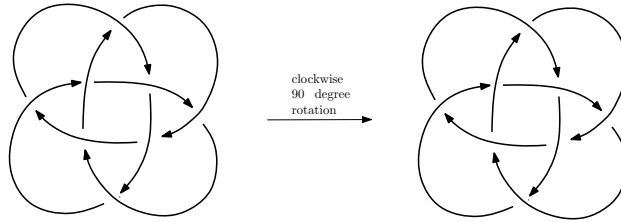


Figure 6.2: Knot(8,18)

See Subsection 6.1.2 for details.

3. Klein bottle.

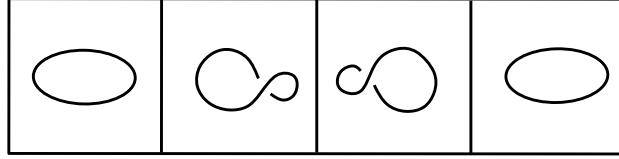


Figure 6.3: Orientation flipping move F_k with positive twist

Let F_k be the cobordism in Figure 6.3, \overline{F}_k be the corresponding close-up surface, then

$$\mathcal{M}(\overline{F}_k) \cong (R/(t-1))^{0,1} \oplus (R/(t+1))^{0,-1}.$$

See Subsection 6.2.1 for details.

4. Interchange components of Whitehead link.

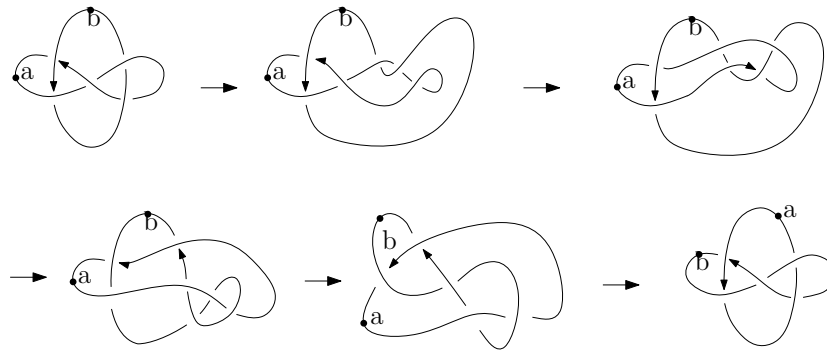


Figure 6.4: Interchange two components of White head link. Some Reidemeister moves are skipped.

Let F_w be the cobordism in Figure 6.4, \overline{F}_w be the corresponding close-

up surface, then

$$\mathcal{M}^{i,j}(\overline{F}_w) = \begin{cases} R/(t-1) & (i,j) = (-3,-8), \text{ or } (-2,-6), \text{ or } (2,4) \\ R/(t+1) & (i,j) = (-2,-4), \text{ or } (-1,-2), \text{ or } (1,0) \\ R/(t+1) \oplus R/(t+1) & (i,j) = (0,-2) \\ R/(t^2-1) & (i,j) = (0,0) \end{cases}$$

See Subsection 6.2.2 for details.

5. Sliding an arc over a link.

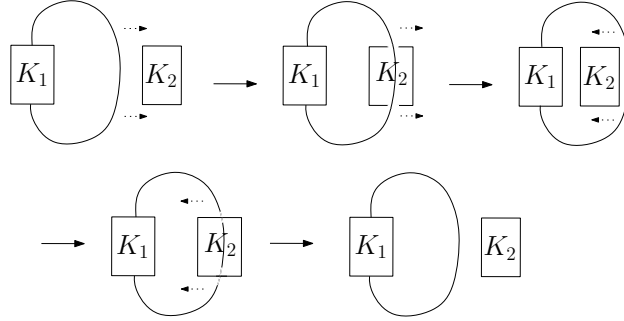


Figure 6.5: Surface obtained by sliding an arc of the link K_1 over another link K_2 and then sliding it back under K_2

Let F_s be the cobordism in Figure 6.5.

Theorem 6.0.2. *The action induced by the cobordism F_s is identity on $Kh(K_1 \cup K_2)$, namely, for all (i, j) , denote by \overline{F}_s the closed surface obtained by gluing two ends of F_s , then*

$$\mathcal{M}^{i,j}(\overline{F}_s) \cong Kh^{i,j}(K_1 \cup K_2) \otimes \mathbb{Q}$$

See Subsection 6.2.3 for details.

6. Surface obtained by surgeries.

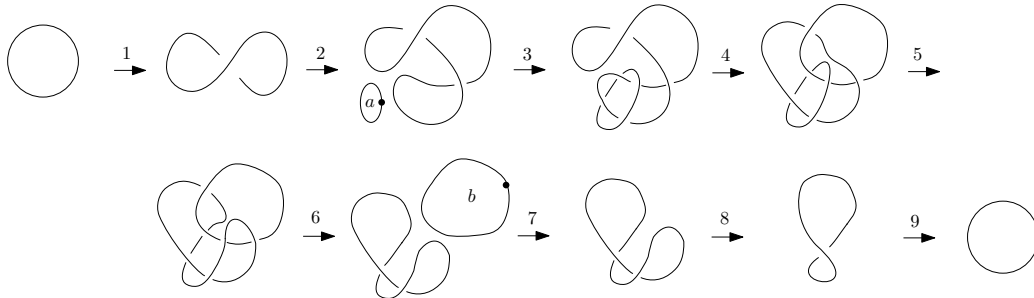


Figure 6.6: A surface F obtained by Reidemeister moves and surgeries

- (a) Let F be the cobordism in Figure 6.6, \overline{F} be the corresponding close-up surface, then

$$\mathcal{M}^{0,j}(\overline{F}) \cong \begin{cases} R/(t-1), & j = 1 \\ R/(t-1), & j = -1 \end{cases}$$

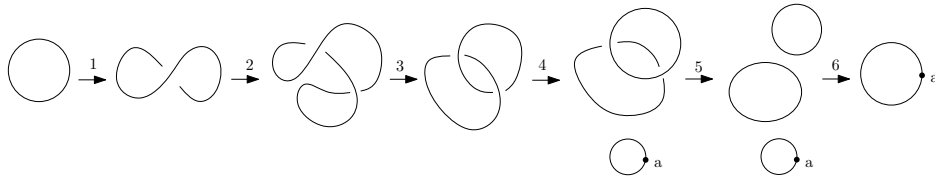


Figure 6.7: A cobordism with one double point, one 1-surgery and three 0, 2-surgeries as well as Reidemeister moves.

(b) Let F_i be the cobordism in Figure, \overline{F}_i be the corresponding close-up surface, then

$$\mathcal{M}^{0,j}(\overline{F}_i) \cong \begin{cases} R/(t-2), & j = 1 \\ 0, & j = -1 \end{cases}$$

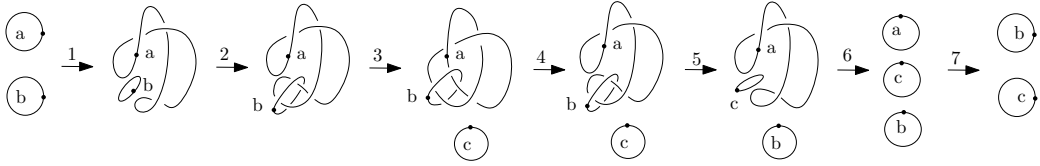


Figure 6.8: Surface obtained by non-orientation-preserving surgery

(c) Let F_n be the cobordism in Figure 6.8, and \overline{F}_n be the corresponding close-up surface, then $\mathcal{M}_{fr}^{p,q}(\overline{F}_n) \equiv 0$

See Subsection 6.3 for details.

The calculation uses the language of tangle cobordisms as in [1]. In other words, all the chain maps between enhanced states are compositions of simple cobordisms. Simple cobordism are cap, cup and saddle surface. In Figure 6.9, notations are in the rectangle box, the meanings are listed below it. We also use “ Id ” to denote the map whose underlying cobordism is just cylinder.

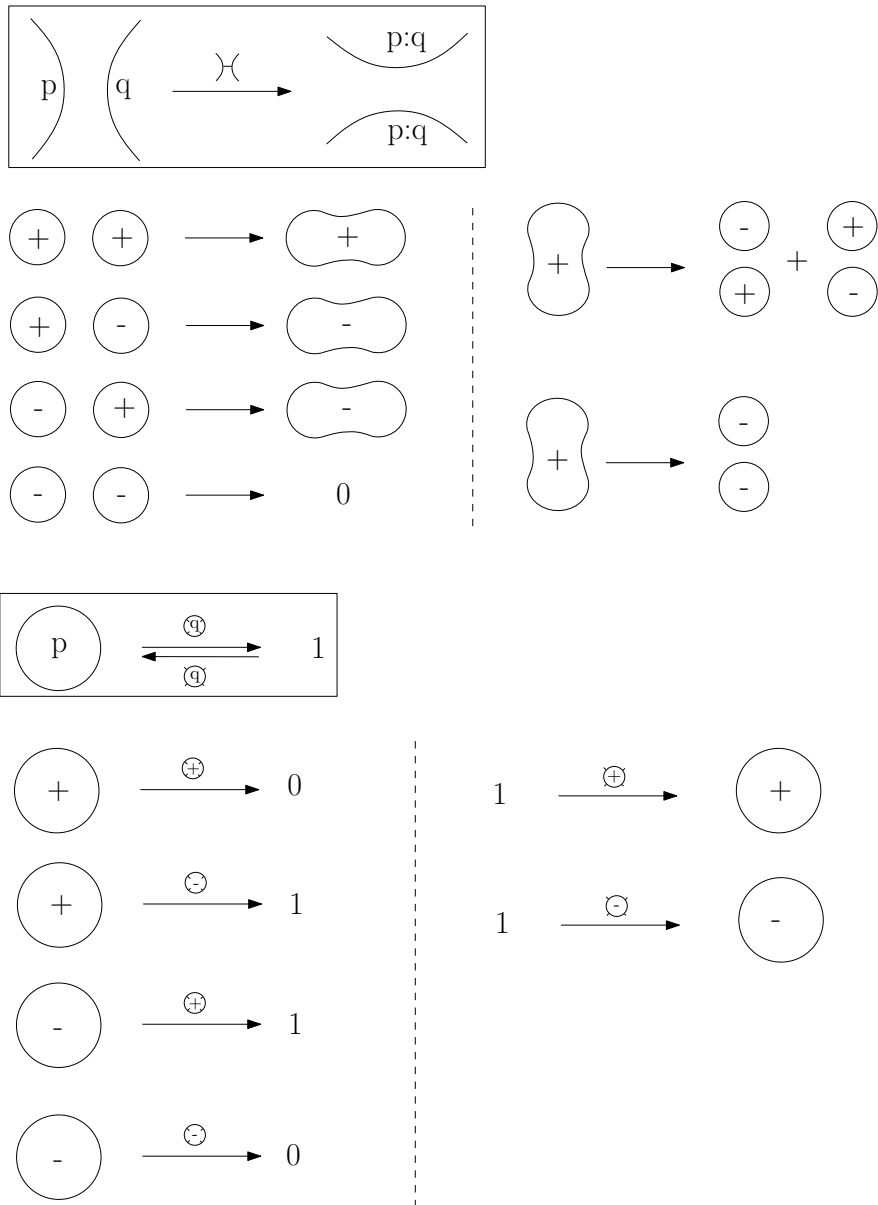


Figure 6.9: Notations for maps for merging two arcs, creation of circles and annihilation of circles.

6.1 Surfaces Obtained by Planer Isotopy

6.1.1 Product Surfaces

Consider the product surface $F = L \times S^1$, where L is an oriented link in S^3 , then $\mathcal{M}(F)$ is just the Khovanov homology of the link together with a trivial \mathbb{Z} action, that is, t acts by identity. In fact, we can cut F at $L \times \{t\}$ with $t \in S^1$ to get a cylinder \tilde{F} , and the invariant is computed by taking the Khovanov homology of \tilde{F} , which is an identity map on Khovanov homology at all gradings. Simply put,

$$\mathcal{M}^{i,j}(F) \cong Kh^{i,j}(L) \otimes \mathbb{Q} \cong (R/(t-1))^{rkKh^{i,j}(L)}.$$

If L is a framed link, then we have

$$\mathcal{M}_{fr}^{p,q}(F) \cong Kh_{fr}^{p,q}(L) \otimes \mathbb{Q} \cong (R/(t-1))^{rkKh_{fr}^{p,q}(L)}.$$

6.1.2 Surfaces Obtained by Rotations

Let L be an oriented link in \mathbb{R}^3 , and D be its diagram. Assume that D has certain rotational symmetry, that is, there is an imaginary center in the diagram D so that a rotation around the center results in a link identical to the original one. We define a surface induced by the rotation as

$$F = L \times [0, 1] /_{L \times \{0\} \sim \rho(L) \times \{1\}}$$

where $\rho : \mathbb{R}^3 \longrightarrow \mathbb{R}^3$ is the corresponding rotation in the 3-space. Moreover, the rotation induces a homomorphism on the Khovanov homology, which can be used to compute $\mathcal{M}(F)$.

Our computation is based on Khovanov homology for oriented links in terms of states and enhanced states as described in Section 2.3. Recall that a state is a distribution of markers for all crossings in a link diagram, and an enhanced state is a state with specified choice (either $+$ or $-$) for each component in a state. In other words, if an ordering is fixed, we can write an enhanced state S as a pair of two vectors,

$$S = [[c_1, c_2, \dots, c_n], [v_1, v_2, \dots, v_m]]$$

where $c_i, v_i = 1$ or 0 , n is the number of crossings, and m is the number of components in each state. The ordering of the second component is induced by the label of edges as illustrated in Figure 6.10. The bi-grading of Khovanov homology (i, j) specifies the state and possible enhanced states.

Now let's consider the simplest example, Trefoil knot, as in Figure 6.1. it is easy to see that the trefoil has a rotational symmetry: rotating the diagram around the center by 120 degree clockwise or counterclockwise results in an identical diagram.

We proved that the rotation induces identity action on Khovanov homology of the trefoil knot.

Corollary 6.1.1. *Let $F_{tref} \equiv T \times [0, 1] /_{T \times \{0\} \sim \rho(T) \times \{1\}}$, where T is the trefoil*

knot, ρ is the rotation, then

$$\mathcal{M}^{i,j}(F_{trefoil}) \cong Kh^{i,j}(T) \otimes \mathbb{Q}.$$

Proof. The Khovanov homology of trefoil has rank 1 in four different gradings:

$$(-3, -9), (0, -1), (0, -3), (-2, -5),$$

and rank 0 for the rest. The generator of each grading can be written as a linear combination of enhanced states. For example, in grading $(-3, -9)$, Khovanov chain complex has only one enhanced state

$$s = [[0, 0, 0], [1, 1, 1]]$$

as depicted in Figure 6.10.

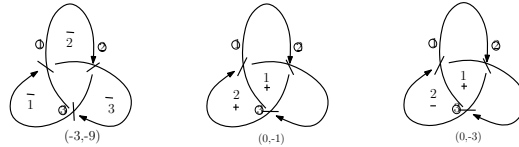


Figure 6.10: Enhanced states of Trefoil on different gradings. Circled numbers indicates the ordering of crossings, numbers without circles defines the ordering of components in a state.

In the chain group $CKh^{-3,9}(T)$, since all components in the enhanced

state are negative, we have

$$0 \longrightarrow CKh^{-3,9}(T) \xrightarrow{d=0} CKh^{-2,-9}(T) .$$

Hence $Kh^{-3,-9}(T)$ is generated by $s = [[0, 0, 0], [1, 1, 1]]$.

On the other hand, we can see that under the rotation, s is unchanged, implying that the rotation induces identity map on $Kh^{-3,-9}(T)$.

Similarly, we can show that $Kh^{0,-1}(T)$ and $Kh^{0,-3}(T)$ are generated by $[[1, 1, 1], [0, 0]]$ and $[[1, 1, 1], [0, 1]]$ respectively, and they are unchanged under the rotation. $Kh^{-2,-5}(T)$ is a little different. Its generator α is a linear combination of two enhanced states rather than a single one.

$$\alpha = -s_1 + s_2$$

where $s_1 = [[1, 0, 0], [0, 1]]$ and $s_2 = [[1, 0, 0], [1, 0]]$. Denote by the same ρ the chain map induced by rotation, then a direct calculation shows that $\rho(s_1) = [[0, 1, 0], [1, 0]]$ and $\rho(s_2) = [[0, 1, 0], [0, 1]]$.

Consider

$$\beta = [[0, 0, 0], [0, 0, 1]] - [[0, 0, 0], [1, 0, 0]].$$

It is easy to show that

$$d\beta = s_2 - s_1 - \rho(s_2) + \rho(s_1).$$

In other words,

$$\rho(\alpha) = \alpha .$$

Since the rotation induces isomorphism, the stabilized map of an isomorphism is itself.

$$\mathcal{M}^{i,j}(F_{trefoil}) \cong Kh^{i,j}(T) \otimes \mathbb{Q}.$$

□

Remark: The mirror image of the trefoil knot has almost the same result except the grading is negated. We also compute torus knots with crossings up to 9, and they all have similar results as the trefoil knot, that is, the action of rotation induces identity map on Khovanov homology.

The first interesting example is from the surface obtained by rotating Knot(8,18) as in Rolfsen Knot Table. In fact, Jacobsson studied the rotation action on Knot(8,18) in [4]. Denote the Knot(8,18) by K , and by F_t the surface obtained by clockwise 90 degree rotation of K around its imaginary center. He calculated the matrix of the action induced by this rotation explicitly on grading (3, 7) and proved that

$$\mathcal{M}(F_t)^{-3,-7} \cong R/(t^3 + t^2 + t + 1).$$

The action on other gradings is not mentioned in his paper. We compute all gradings, and it turns out that the rotation action is non-trivial in many other gradings as well.

Corollary 6.1.2. $\mathcal{M}^{i,j}(F_t)$ admits a nontrivial R action on $Kh^{i,j}(K)$ if the Betti number of $Kh^{i,j}(K)$ is larger than 1.

The proof is also based on direct computation. For each grading, we choose a basis for Khovanov homology in terms of linear combinations of enhanced states, then compute the image under the rotation and compare the image with the basis gives a matrix.

The computation complexity of Khovanov homology increases exponentially when the number of crossings increases. Thanks to KnotTheory¹ and KhoHo², we can compute all the ³ranks of the Khovanov homology of a given link diagram.

For example, the Khovanov chain complex for Knot(8,18) is the following

¹KnotTheory is a Mathematica Package for computing knot invariants including Khovanov homology by Dror Bar-Natan

²KhoHo is a program for computing the Khovanov homology by Alexander Shumakovitch

³Torsions can be computed as well, but it not needed here

(obtained by KhoHo)

i/j	-4	-3	-2	-1	0	1	2	3	4
9	0	0	0	0	0	0	0	0	1
7	0	0	0	0	0	0	0	8	5
5	0	0	0	0	0	4	28	32	10
3	0	0	0	4	25	68	84	48	10
1	1	8	28	68	120	128	84	32	5
-1	5	32	84	128	120	68	28	8	1
-3	10	48	84	68	25	4	0	0	0
-5	10	32	28	4	0	0	0	0	0
-7	5	8	0	0	0	0	0	0	0
-9	1	0	0	0	0	0	0	0	0

The Betti number of its Khovanov homology is

i/j	-4	-3	-2	-1	0	1	2	3	4
9	0	0	0	0	0	0	0	0	1
7	0	0	0	0	0	0	0	3	0
5	0	0	0	0	0	0	3	1	0
3	0	0	0	0	0	4	3	0	0
1	0	0	0	0	5	3	0	0	0
-1	0	0	0	3	5	0	0	0	0
-3	0	0	3	4	0	0	0	0	0
-5	0	1	3	0	0	0	0	0	0
-7	0	3	0	0	0	0	0	0	0
-9	1	0	0	0	0	0	0	0	0

However, it is still not easy to compute cycles of Khovanov homology, let alone the generators in terms of enhanced states. For example, in grading $(-2, -3)$, we see that the rank of the chain complex is 84, while the rank of the Khovanov homology is only 3. To find cycles, it involves computing the kernels of a the differential matrix that is not in the image of the previous differential matrix.

Both program mentioned above help us find the rank of Khovanov homology, but they do not compute the generators for the homology. However, they do provide all the necessary information to find generators of the ho-

mology. In our computation, we use the information obtained by KhoHo and extend KhoHo to compute the explicit generators of Khovanov homology and the induced maps of cobordisms. The codes can be found in the Appendix B.

Proof. We compute the list of $\mathcal{M}(F_t)$ for all gradings

$$\mathcal{M}^{i,j}(F_t) \cong \begin{cases} R/(t-1) & (i, j) = \pm(4, 9), \pm(3, 5) \\ R/(t^3 + t^2 + t + 1) & (i, j) = \pm(3, 7), \pm(2, 3) \\ R/(t^3 - t^2 + t - 1) & (i, j) = \pm(2, 5), \pm(1, 1) \\ R/(t^4 - 1) & (i, j) = \pm(1, 3) \\ R/(t^4 - 1) \oplus R/(t + 1) & (i, j) = (0, \pm 1) \\ 0 & \textit{otherwise} \end{cases}$$

It is not difficult to see from the list above that the rotation acts on grading $\pm(4, 9)$ and $\pm(3, 5)$ by identity, while for other gradings whose rank are more than 1, the rotation action is quite nontrivial.

□

Remarks: There are several other surfaces obtained by rotations, like Borromean Ring, $Knot(5, 1)$, $Knot(7, 1)$, $Knot(10, 123)$ and so on. They all can be computed by our program. The results can be found in the Appendix C.

So far we have seen surfaces obtained by planer isotopies. In the following sections, we will see examples obtained by Reidemeister moves.

6.2 Surfaces Obtained by Reidemeister Moves

6.2.1 Klein Bottle

Klein bottle can be obtained by identifying two circles along the orientation reversing map, which can be realized as a composition of first Reidemeister moves as in Figure 6.3.

In Khovanov homology, we have explicit chain maps induced by Reidemeister moves as described in [1] and [4]. Since Khovanov homology of the unknot doesn't depend on the orientation, we can simply identify two unknots with opposite orientations.

Klein bottle can be seen as a composition of two first Reidemeister moves with positive twist as in Figure 6.3, the corresponding chain map of which is shown in Figure 6.11.

$$\begin{array}{ccc}
 \boxed{\text{positive twist} \rightarrow \text{negative twist}} & & \boxed{\text{negative twist} \rightarrow \text{positive twist}} \\
 \text{positive twist} \xrightarrow{\oplus} 0, \quad \text{negative twist} \rightarrow 0 & & \text{negative twist} \rightarrow \text{positive twist} - \text{negative twist} \\
 \text{positive twist} \xrightarrow{\oplus} \text{positive twist} & & \text{negative twist} \xrightarrow{\ominus} \text{negative twist}
 \end{array}$$

Figure 6.11: Chain map induced by the first Reidemeister move with positive kink. p means $+$ or $-$.

$Kh^{*,*}(\bigcirc)$ can be identified with a 2-dimensional vector space with basis $v_+ =$ positive circle and $v_- =$ negative circle in the enhanced state. We have

$$\begin{aligned} \bigcirc_+ &\rightarrow \bigcirc_+ \circlearrowleft - \bigcirc_- \circlearrowright \rightarrow \bigcirc_+ \circlearrowright - \bigcirc_- \circlearrowleft \rightarrow - \bigcirc_+ \\ \bigcirc_- &\rightarrow \bigcirc_- \circlearrowleft \rightarrow \bigcirc_- \circlearrowright \rightarrow \bigcirc_- \end{aligned}$$

Direct computation shows

$$Kh^{0,j}(F_k) = \begin{cases} -1 & j = 1 \\ 1 & j = -1 \end{cases}$$

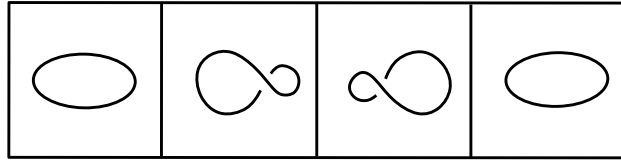


Figure 6.12: Orientation flipping move F'_k with negative twist

Klein bottle can also be seen as a composition of two first Reidemeister moves with negative twist as in Figure 6.12, the corresponding chain map of which is shown in Figure 6.13.

$$\begin{aligned} \bigcirc_+ &\rightarrow \bigcirc_+ \circlearrowleft \rightarrow \bigcirc_+ \circlearrowright \rightarrow \bigcirc_+ \\ \bigcirc_- &\rightarrow \bigcirc_- \circlearrowleft \rightarrow \bigcirc_- \circlearrowright \rightarrow - \bigcirc_- \end{aligned}$$

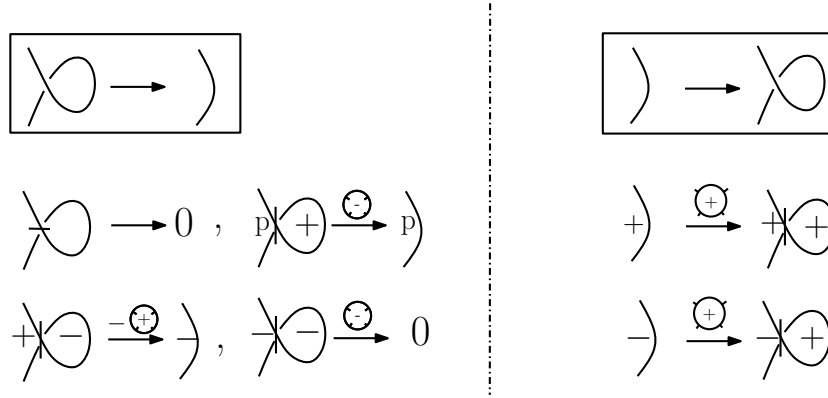


Figure 6.13: First Reidemeister move with negative twist

It can be easily obtained that

$$Kh^{0,j}(F'_k) = \begin{cases} 1 & \text{if } j = 1 \\ -1 & \text{if } j = -1 \end{cases}$$

In summary,

$$\mathcal{M}(F_k) \cong (R/(t-1))^{0,1} \oplus (R/(t+1))^{0,-1}.$$

This invariant can distinguish Klein Bottle from the standard embedding of torus in $S^3 \times S^1$. In fact, let T be the standardly embedded torus in $S^3 \times S^1$, then

$$\mathcal{M}(T) \cong (R/(t-1))^{0,1} \oplus (R/(t-1))^{0,-1}.$$

6.2.2 Interchange component of Whitehead link

Let W be the whitehead link whose two components labeled by a and b respectively. These two components can be interchanged using Reidemeister moves as depicted in Figure 6.4.

Denote by F_w the surface obtained by this move, then $Kh(F_w)$ can be computed explicitly using all three Reidemeister moves. Since the two ends of F_s are identical even with orientation, we can close it up to obtain a surface denote by \overline{F}_w , then

$$\mathcal{M}^{i,j}(\overline{F}_w) = \begin{cases} R/(t-1) & (i, j) = (-3, -8), \text{ or } (-2, -6), \text{ or } (2, 4) \\ R/(t+1) & (i, j) = (-2, -4), \text{ or } (-1, -2), \text{ or } (1, 0) \\ R/(t+1) \oplus R/(t+1) & (i, j) = (0, -2) \\ R/(t^2-1) & (i, j) = (0, 0) \end{cases}$$

Remark. In this example, we can see that our invariant can detect some kind of "knotting" in the surface obtained by interchanging components of a link digram using Reidemeister moves. Similar results can be found for other links, for example, Hopf link.

6.2.3 Second and Third Reidemeister moves

In this section, we will see some weakness of our invariant. More precisely, let K_1 and K_2 be two link diagrams, we can slide an arc of K_1 over K_2 , then slide it back, the resulting diagram is identical to the starting one. This

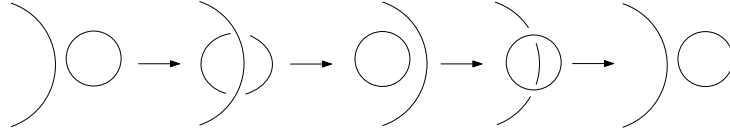
isotopy defines a cobordism F_s with two identical boundary components, so a surface \overline{F}_s can be obtained by gluing these two boundary components. See Figure 6.5.

Theorem 6.2.1. *The action induced by F_s is identity on $Kh(K_1 \cup K_2)$, namely, for all (i, j) ,*

$$\mathcal{M}^{i,j}(\overline{F}_s) \cong Kh^{i,j}(K_1 \cup K_2) \otimes \mathbb{Q}$$

Proof. The proof is based on the observation of the chain maps induced by the second and the third Reidemeister moves.

First, let's consider a special case when K_2 is unknot.



To prove the theorem for this case, we need to apply several compositions of second Reidemeister moves. The chain map induced by the second Reidemeister move is shown in Figure 6.14. The right hand side map is just the inverse map of the left hand side, and vice versa.

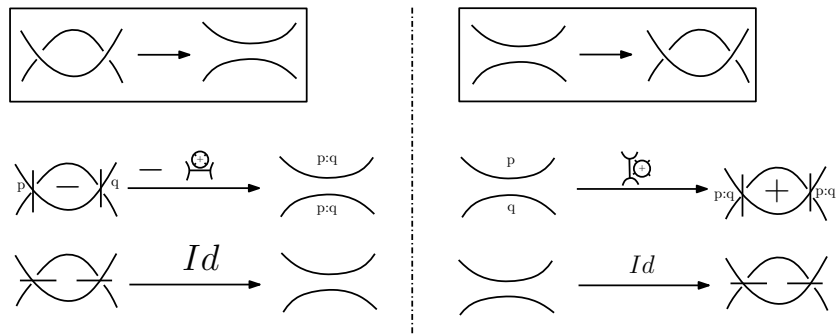
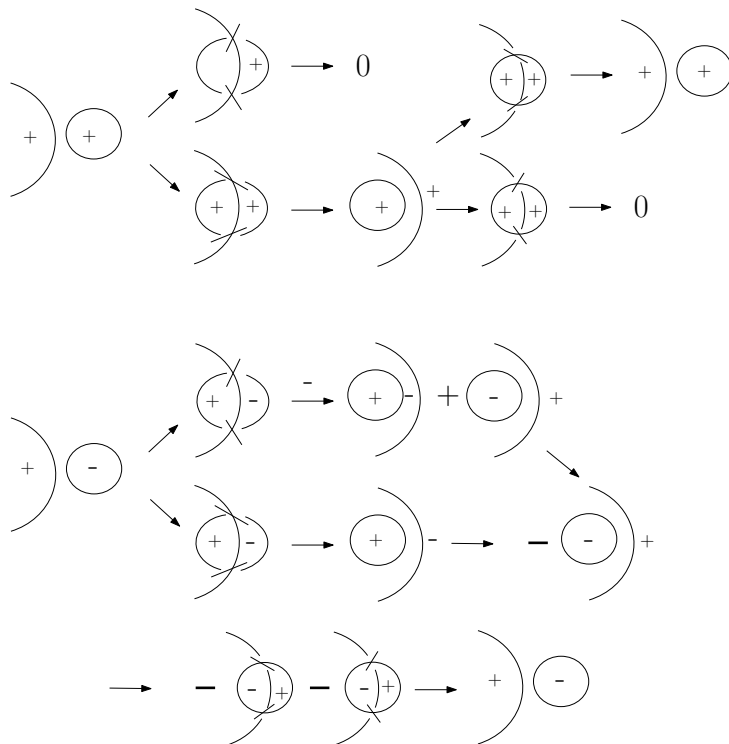
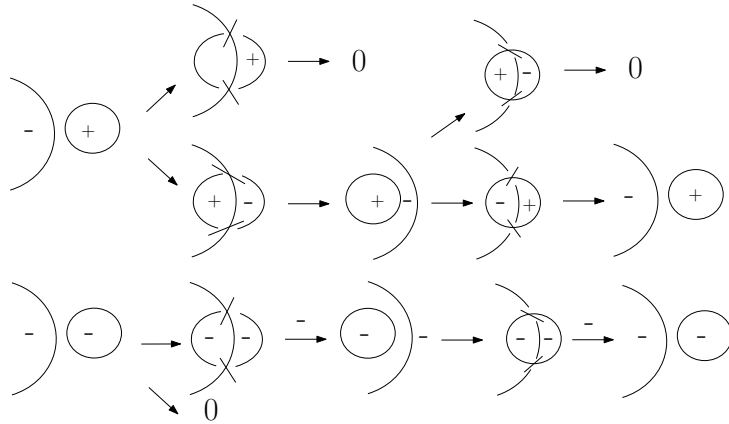


Figure 6.14: Chain maps induced by the second Reidemeister move.

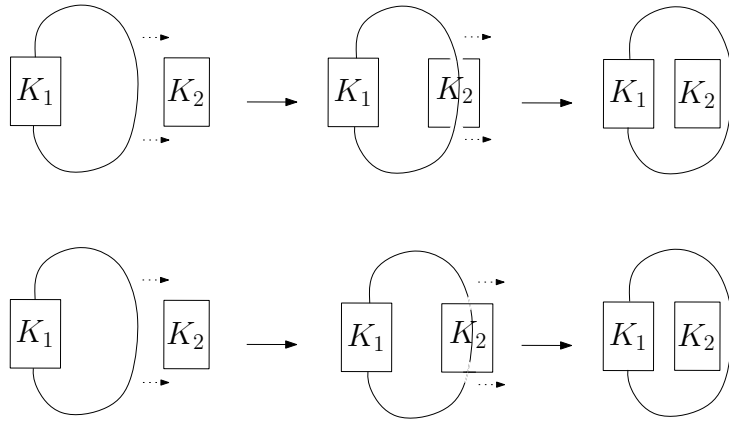
Using the chain map in Figure 6.14, we have the following





which shows that the action induced by F_s is identity on chain level and hence on Khovanov homology.

In general, if K_2 is a link diagram with at least one crossing, it is equivalent to show that the following two moves induce the same map on homology:



This reduces to compare two types third Reidemeister moves in Figure 6.15 and Figure 6.16.

It's proved by Bar-Natan in [1] and Clark, Morrison and Walker in [2] that chain maps induced by Reidemeister moves are unique up to chain homotopy

and ± 1 multiples in the appropriate grading. This property makes it possible to choose alternative chain maps for Reidemeister moves.

Consider two types of third Reidemeister move in Figure 6.15, we choose chain maps for each type so that they map each state to the same state. The detailed calculation can be found in the Appendix D.

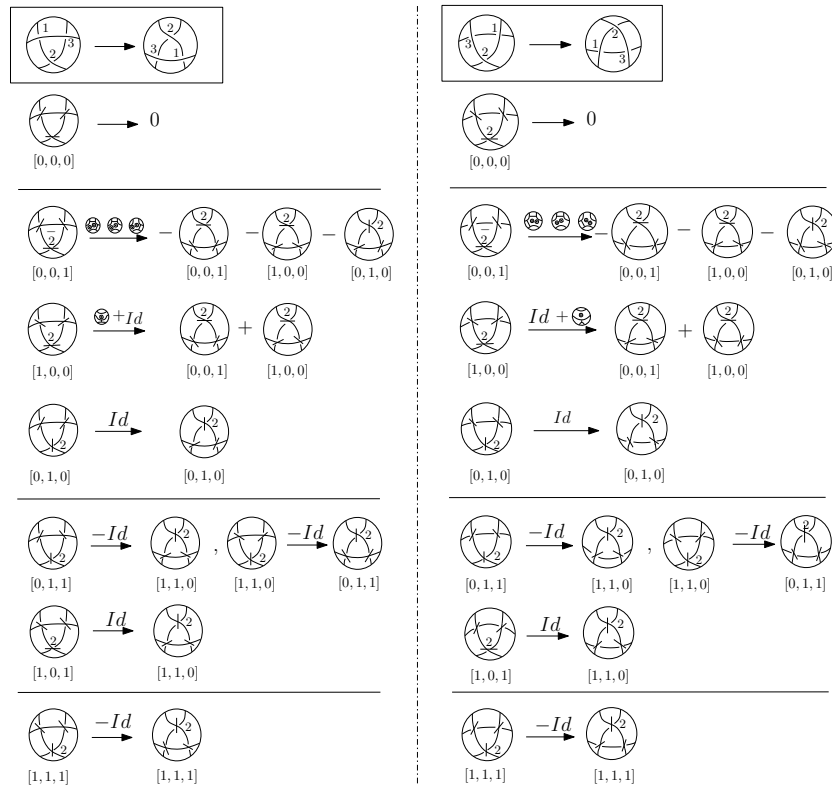


Figure 6.15: Compare of chain maps induced by two third Reidemeister moves with state information.

For another two types of third Reidemeister moves we have similar result as in Figure 6.16.

By comparing chain maps above, we can see that after sliding the arc

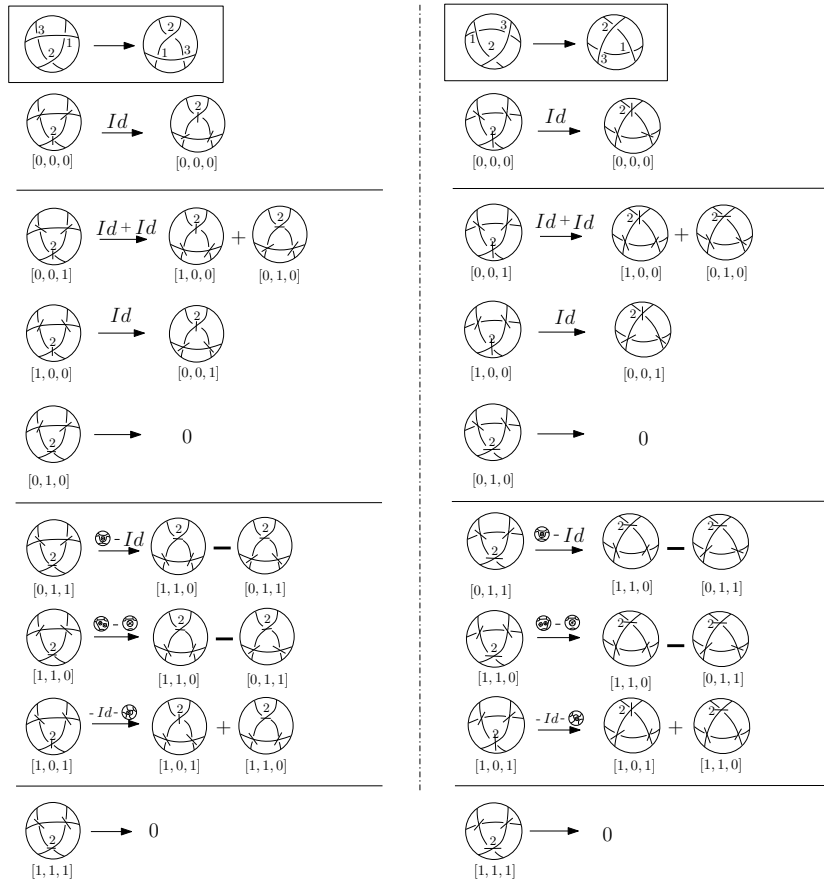


Figure 6.16: Compare of chain maps induced by another two third Reidemeister moves

over or under the whole link diagram, the states are preserved. In fact, when the arc slide over a crossing over or under, the marker of that crossing is either preserved or changed from positive marker to negative marker, but not from negative marker to positive marker. Thus after sliding the arc over or under the whole link diagram K_2 , the markers of all crossings has to be the same due to the grading reason. Moreover, maps that preserve marker of

the crossings induces the same map on enhanced states for both under and over slide.

In other words, the chain map induced by F_s acts by ± 1 on the Khovanov chain, while this is not enough to show that $\mathcal{M}(\overline{F}_s)$ is identity since it is possible that for some (i, j) , $Kh^{i,j}(F_s) = Id$, while for others $Kh^{i,j}(F_s) = -Id$. Fortunately this possibility can be excluded by the following observation. In Figure 6.15, the sign of the chain map is defined for each state, not enhanced state, suppose $f_{i,j} = CKh^{i,j}(F_s) = Id$, we have the following diagram commutes:

$$\begin{array}{ccc} [c_1, c_2, \dots, c_i, \dots, c_n] & \xrightarrow{f^{i,j}} & [c_1, c_2, \dots, c_n] \\ \downarrow d_k & & \downarrow d_i \\ (-1)^{s_k} [c_1, c_2, \dots, dc_k, \dots, c_n] & \xrightarrow{f_k^{i-1,j}} & (-1)^{s_k} [c_1, c_2, \dots, dc_k, \dots, c_n] \end{array}$$

where d_k is the k -th differential, s_k is sum of 1's after c_k , hence $f_k^{i-1,j} = Id$ for any k . In particular, if a chain map f is identity on $[0, 0, \dots, 0]$, then the above argument shows that f is identity on all states. Since our invariant is well-defined up to sign, the action induced by F_s is identity on $Kh^{i,j}(K_1 \cup K_2)$, which completes the proof. \square

Remark. So far all the examples listed above are obtained by Reidemeister moves or planner isotopies. As discussed in Section 4.3, we get results for framed version simply by replacing $\mathcal{M}^{i,j}$ with $\mathcal{M}_{fr}^{p,q}$, where (p, q) and (i, j)

satisfying

$$p(S) = j(S) - i(S) - w(D) - fr(D), \quad q(S) = -2j(S) + 3w(D) + 3fr(D),$$

In the following section, we will see that the original version and the framed version of Khovanov homology have different results.

6.3 Examples using surgeries

In this section, we consider surfaces obtained by 0, 1, 2-surgeries together with Reidemeister moves.

Recall that the immersed link cobordism induces the following map on Khovanov homology

$$Kh^{i,j}(D_0) \longrightarrow Kh^{i+2d_2, j-2d_1+4d_2+\chi(F)}(D_1).$$

There are two sources of grading change:

1. **i-surgeries, where i=0,1,2.**

0,2-surgery (creating or annihilating a 2-disc) changes the grading by a positive multiple of $(0, 1)$, while 1-surgery changes the grading by a positive multiple of $(0, -1)$.

2. **Double points.**

Recall that in Section 3.1 there are two types of double points in a

immersed cobordism depending on the local orientation. Type 1 double points ($\nearrow \searrow \rightarrow \searrow \nearrow$) change the grading by a positive multiple of $(0, -2)$, while type 2 double points change ($\nearrow \searrow \rightarrow \nearrow \searrow$) the grading by a positive multiple of $(2, 4)$.

To obtain possible nontrivial result, we need cobordisms satisfying

$$2d_2 = 0, \chi(F) - 2d_1 = 0.$$

In terms of double points and surgeries, we need cobordisms that admit no Type 2 double points. If there is a Type 1 double point, there must be some 0,2-surgeries which can cancel the effect of grading change by Type 1 double point. If there is no double points, the number of 1-surgery has to be the same as that of 0,2-surgery. One example is shown in Figure 6.6.

We use movie representation to illustrate this cobordism F in Figure 6.6, in which moves are labeled from 1 to 9 and some circle components are labeled by a, b. Move 1 is the just the first Reidemeister move. Move 2 is first move together with creation of a circle or 0-surgery. Move 3 moves the circle a by second Reidemeister moves. Move 4 performs a 1-surgery on the same component. Move 5 performs another 1-surgery. Move 6 moves circle b away from the other component. Move 8 kills circle b by 2-surgery. Move 8 and 9 are just first Reidemeister moves. The grading is preserved since the number of 1-surgeries is equal to the number of 0,2-surgeries.

Denote by K the unknot, by v_+ the positive circle, by v_- the negative

one, then

$$Kh^{0,j}(K) \cong \begin{cases} \langle v_+ \rangle, & j = 1 \\ \langle v_- \rangle, & j = -1 \end{cases}$$

Apply Khovanov homology to the surface F we have

$$Kh^{0,j}(F) = \begin{cases} 1, & j = 1 \\ 1, & j = -1 \end{cases}$$

Denote by \overline{F} the closed surface obtained by identifying two ends of F , then

$$\mathcal{M}^{0,j}(\overline{F}) \cong \begin{cases} R/(t-1), & j = 1 \\ R/(t-1), & j = -1 \end{cases}$$

Another example is shown in Figure 6b .

After adding two positive twists to a circle, a 1-surgery is performed to get a Hopf link. A double point is added by a crossing change. Meanwhile, a circle is added to the link by 0-surgery. Then a second Reidemeister move is used to separate the two circles. Finally these two components are killed by two 2-surgeries. Notice that the cobordism obtained in Figure 6b has a double point obtained by Move 4. Denote by \overline{F} again the closed surface obtained by gluing two ends. We have

$$\mathcal{M}^{0,j}(\overline{F}) \cong \begin{cases} R/(t-2), & j = 1 \\ 0, & j = -1 \end{cases}$$

For framed Khovanov homology, we have

$$Kh_{fr}^{p,q}(D_0) \longrightarrow Kh_{fr}^{p+\chi(F)-e, q-2\chi(F)+3e-2d}(D_1).$$

There are several sources contributing to the change of grading:

1. **i -surgeries, where $i = 0, 1, 2$.**

0, 2-surgeries change the (p, q) -grading by $(1, -2)$, while 1-surgery change the grading by $(-1, 2)$. Denote the number of these surgeries by S_i .

2. **Double points.**

Adding a double point will change the grading by $(0, -2)$, denote the number of double points by n_d .

3. **Framing change.**

We can always change $fr(D)$ of a link to an arbitrary framing by a cylinder. Namely, let L_0 be a framed link with total framing $a \in \mathbb{Z}$, $b \in \mathbb{Z}$ be another total framing of L_0 . Then we can change the framing of L_0 from a to b by a product cobordism $F = L_0 \times [0, 1]$. The framing change occurs during this trivial cobordism. The grading changes by a multiple of $(1, -3)$ as discussed in Section 4.3. We denote the number of such change by fr .

Notice that S_i, n_d are non-negative integers and fr is any integer. Together

with $\chi(F) = e$ and $2\chi(F) + 2d = 3e$, we have

$$(S_0 + S_2)(1, -2) + S_1(-1, 2) + n_d(0, -2) + fr(1, -3) = 0,$$

which implies that

$$S_0 + S_2 - S_1 = -fr$$

$$fr = -2n_d.$$

In other words, we need two extra 0, 2-surgeries to cancel one double point.

Also, notice that if

$$S_1(-1, 2) + n_d(0, -2) + fr(1, -3) = 0,$$

then

$$S_1 = fr, \quad S_1 = -2dp.$$

On the other hand, since $S_1 \geq 0$ and $n_d \geq 0$, the effect of 1-surgery cannot be canceled by a combination of double points and framing changes.

Then

$$\mathcal{M}_{fr}^{p,q}(\overline{F}) \cong \begin{cases} R/(t-2) & p = 1, \quad q = -2. \\ 0 & \text{otherwise} \end{cases}$$

Notice that one move is omitted at the end of the cobordism, namely the cylinder which changes $fr(D)$ by $(-2, 6)$.

Besides, framed Khovanov homology can be applied to non-orientation-

preserving surgeries as well. See Figure 6.8.

Denote by \overline{F} again the surface obtained by gluing the two ends of the surface in Figure 6.8. Unfortunately, the invariant $\mathcal{M}_{fr}^{p,q}(\overline{F}) \equiv 0$.

Remarks. Similar examples can be obtained by performing the opposite twists on Move 1 and 2 in Figure 6.6 and 6b. Also notice that the surgery performed in above examples using immersed Khovanov homology are orientation-preserving. For non-orientation-preserving surgeries, it is not well-defined for the Khovanov homology. However, we don't have this problem in the framed version.

Chapter 7

Generically Immersed Surfaces in S^4

It is well-known that $S^3 \times S^1$ can be obtained by a surgery along a standardly embedded S^2 in S^4 by cutting out the neighborhood of this S^2 and gluing back with a $D^3 \times S^1$, where D^3 is the 3-dimensional disc. This can be used to define invariants of pairs (S, F) in S^4 , where S is the standardly embedded 2-sphere, and F is a generically immersed surface transversely intersecting S in S^4 . Such pairs are considered up to ambient isotopy. Denote such pair by $S^2 \cup F$.

Then for $S^2 \times \{point\} \subset S^2 \times D^2$,

$$|F \cap (S^2 \times \{point\})| = n.$$

In other words, F intersects the copy of the standard S^2 at the same number of points.

Besides, since the complement of the neighborhood of the standard S^2 is $D^3 \times S^1$, the transversal intersection $F \cap (D^3 \times \{point\})$ is thus a tangle with n boundary points $\{p_1, p_2, \dots, p_n\}$. Here we use the same collection of points to represent the intersection in each copy of S^2 . Recall that we cut out the neighborhood of the standard S^2 and glue back another copy of $D^3 \times S^1$. Eventually what we obtain from F is no longer a closed surface in $S^3 \times S^1$ since in each slice $S^3 \times \{point\}$ we only have a tangle instead of a link with tangle sitting inside one hemisphere of S^3 . To have a closed surface, we need to close up the tangles using extra arches in the other hemisphere of S^3 . In general, there is no unique way to close up a tangle. One way is to consider all possible ways to close up the tangle. That's related to a version of Khovanov homology of tangles by Khovanov in [7]. For a special case $n = 2$, there is only one way to close up the tangle. Hence we have a unique closed surface generically immersed in $S^3 \times S^1$. By applying the surface invariant \mathcal{M} and \mathcal{M}_{fr} , we have two surface invariants in S^4 up to ambient isotopy.

Theorem 7.0.1. *If $|F \cap S^2| = 2$, $\mathcal{M}(F)$ and $\mathcal{M}_{fr}(F)$ are invariants of $S^2 \cup F$ up to ambient isotopy.*

Proof. Let $F' \subset S^4$ be another generically immersed surface such that $(S^2 \cup F)$ and $(S^2 \cup F')$ are *ambient isotopic* in S^4 , that is, there exists a family of diffeomorphisms

$$H : S^4 \times [0, 1] \longrightarrow S^4$$

such that

$$H(x, 0) = x, \quad H(S^2 \cup F, 1) = S^2 \cup F'.$$

Denote by the same F and F' the new surfaces in $S^3 \times S^1$ obtained by closing up the tangle. The isotopy in S^4 gives an ambient isotopy of F and F' in $S^3 \times S^1$. By Theorem 5.2.1 and Theorem 5.2.1, the theorem is proved. \square

Examples can be obtained by spinning and twisting in S^4 . Let K be a knotted embedded in a three ball $B^3 = \{x \in \mathbb{R}^3 \mid |x| \leq 1\}$. When B^3 is rotated around the standard S^2 in S^4 , the continuous trace of K forms a locally flat 2-sphere or 2-knot. This 2-knot is said to be derived from K by *spinning*. If we twist the arc K m times while it spins, another 2-knot in S^4 is obtained which is said to be derived from k by *m -twist spinning*.

The computation for these examples are similar as in Section 6.

Bibliography

- [1] Dror Bar-Natan. *Khovanov's homology for tangles and cobordisms*. Gemetry and Topology, Volume 9 (2005) 1443-1499
- [2] David Clark, Scott Morrison, and Kevin Walker. *Fixing the functoriality of Khovanov homology*. arXiv:701339v2, 21 Jan 2008.
- [3] Patrick M.Gilmer. *Invariants for one-dimensional cohomology classes arising from TQFT* Topology and its Applications 75(1997 217-259)
- [4] Magnus Jacobsson. *An invariant of link cobordisms from Khovanov homology*. Algebraic & Geometric Topology, Volume 4 (2004) 1211C1251
- [5] Antoni A. Kosinski. *Differential manifolds*. Volume 138 (Pure and Applied Mathematics), pp. 36
- [6] Mikhail Khovanov. *A categorification of the Jones polynomial*. Duke Math. J. 101 (2000), no. 3, 359–426.
- [7] Mikhail Khovanov. *An invariant of tangle cobordisms*. Trans. Amer. Math. Soc. 358 (2006), 315-327, arXiv:math.QA/0207264..

- [8] Dennis Roseman. *Reidemeister-type moves for surfaces in four dimensional space.* in Banach Center Publications 42, Knot Theory (1998), 347380.
- [9] Jacob Rasmussen. *Khovanov's invariant for closed surfaces.* arXiv:math.GT/0502527, 24 Feb 2005.
- [10] Alexander Shumakovitch. *KhoHo.* <http://www.geometrie.ch/KhoHo/>.
- [11] J Scott Carter, Masahico Saito. *Reidemeister moves for surface isotopies and their interpretations as moves to movies.* Knot Theory Ramifications 2 (1993) 251284.
- [12] Kokoro Tanaka. *Khovanov-jacobsson numbers and invariants of surface-knots derived from Bar-Natan's theory.* Proceedings of the American Mathematical Society , Volume 134, Number 12, December 2006.
- [13] Hassler Whitney. *On the topology of differentiable manifold.* University of Michigan Lectures, 1941, 101-141.
- [14] Oleg Viro. *Khovanov homology, its definitions and ramifications.* Fundamenta Mathematicae,184(2004).

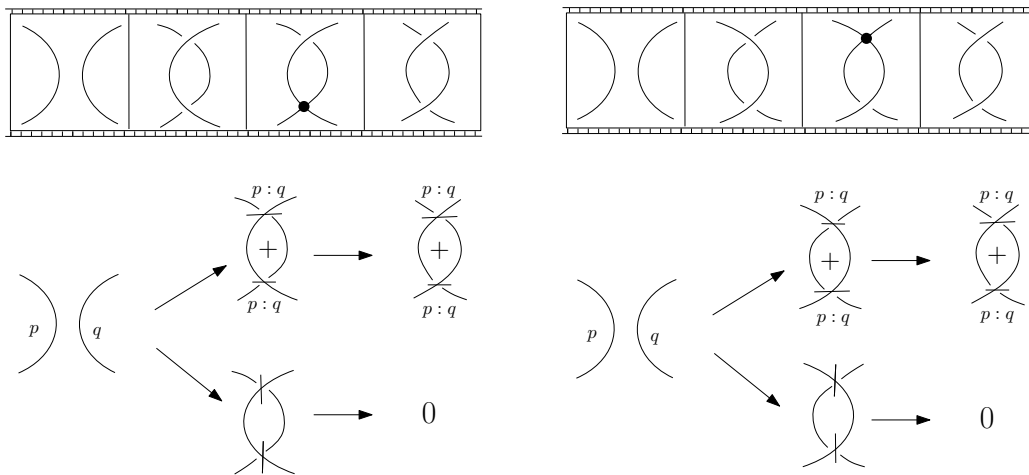
Appendix A

Calculations on Extra Movie

Moves

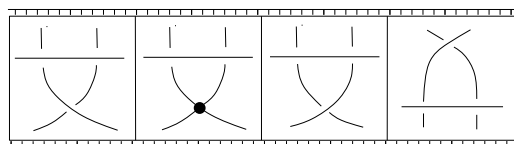
There are two extra movie moves as in Figure 3.1: Movie Move 16 and 17. In both Movie Moves, movies on two sides induce chain maps on Khovanov chain complex. These maps are the composition of the crossing change map and maps induced by Reidemeister moves. The calculation on Movie Move

16 is shown below.



We can see that both movies induced the same map on chain level.

Similarly, in Movie Move 17, we calculate the induced maps as below.



$$\begin{array}{l}
 \begin{array}{c} 3 \quad | \quad | \quad 1 \\ \diagdown \quad \diagup \\ \text{---} \\ \diagup \quad \diagdown \\ 2 \end{array} \rightarrow \begin{array}{c} 3 \quad | \quad | \quad 1 \\ \diagdown \quad \diagup \\ \text{---} \\ \diagup \quad \diagdown \\ 2 \end{array} \rightarrow 0 \\
 \\
 \begin{array}{c} 3 \quad | \quad | \quad 1 \\ \diagdown \quad \diagup \\ \text{---} \\ \diagup \quad \diagdown \\ 2 \end{array} \xrightarrow{-} \begin{array}{c} 3 \quad | \quad | \quad 1 \\ \diagdown \quad \diagup \\ \text{---} \\ \diagup \quad \diagdown \\ 2 \end{array} \xrightarrow{-} \begin{array}{c} 2 \\ \diagdown \quad \diagup \\ \text{---} \\ \diagup \quad \diagdown \\ 1 \quad | \quad | \quad 3 \end{array} \quad \text{---} \quad \begin{array}{c} 2 \\ \diagdown \quad \diagup \\ \text{---} \\ \diagup \quad \diagdown \\ 1 \quad | \quad | \quad 3 \end{array} \\
 \\
 \begin{array}{c} 3 \quad | \quad | \quad 1 \\ \diagdown \quad \diagup \\ \text{---} \\ \diagup \quad \diagdown \\ 2 \end{array} \rightarrow \begin{array}{c} 3 \quad | \quad | \quad 1 \\ \diagdown \quad \diagup \\ \text{---} \\ \diagup \quad \diagdown \\ 2 \end{array} \xrightarrow{-} \begin{array}{c} 2 \\ \diagdown \quad \diagup \\ \text{---} \\ \diagup \quad \diagdown \\ 1 \quad | \quad | \quad 3 \end{array} \quad \text{---} \quad \begin{array}{c} 2 \\ \diagdown \quad \diagup \\ \text{---} \\ \diagup \quad \diagdown \\ 1 \quad | \quad | \quad 3 \end{array} \\
 \\
 \begin{array}{c} 3 \quad | \quad | \quad 1 \\ \diagdown \quad \diagup \\ \text{---} \\ \diagup \quad \diagdown \\ 2 \end{array} \rightarrow \begin{array}{c} 3 \quad | \quad | \quad 1 \\ \diagdown \quad \diagup \\ \text{---} \\ \diagup \quad \diagdown \\ 2 \end{array} \rightarrow 0 \quad , \quad \begin{array}{c} 3 \quad | \quad | \quad 1 \\ \text{---} \\ \diagdown \quad \diagup \\ 2 \end{array} \rightarrow 0
 \end{array}$$

Appendix B

A Program to Compute Khovanov Homology

B.1 Introduction to KhoHo.

KhoHo is computer program written by Alexander Shumakovitch [10] using the algebraic system PARI/GP. The input is an oriented link diagram which is a directed graph with labeled edges and vertices. It is represented by a $n \times 4$ matrix, where n is the number of crossings. At each crossing, there is an entering edge, which is one of the edge on the over-crossing and moving towards the vertex. If we start with this edge and go clockwise around the crossing we see four edges in order. Place these four number in the same order in a row vector as a row of the matrix. So each row corresponds to a

crossing with the first entry as the entering edge. The order of the crossing is thus the order of rows.

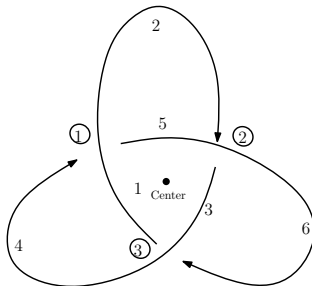


Figure B.1: Diagram of trefoil knot

For example, in Figure B.1, the diagram matrix is

$$\begin{pmatrix} 1 & 4 & 2 & 5 \\ 5 & 2 & 6 & 3 \\ 3 & 6 & 4 & 1 \end{pmatrix}$$

Khovanov homology can be computed in terms of states and enhanced states as described in the section 2.3. One way to realize it is using vectors. More precisely, let L be a link diagram with n crossings, we can assign a vector S of three components to each enhanced state, each component of which is itself a vector.

$$S = [s, \text{ens}, \text{edge}]$$

The first component s is a binary vector (a vector with entry 1 or 0 only), of length n , which corresponds to a state with 0 representing 0-smoothing

or positive marker \times , 1 representing 1-smoothing or negative marker \times . The second component ens is a vector of length m where m is the number of components for each state s . It is also a binary vector, with 0 representing positive circle, 1 representing negative circle. The last component is vector of increasing integers with each integer representing the smallest edge (according to the label of each edge) of each component in the enhanced state. For example, in Figure 6.10, the first picture corresponds to a vector

$$S_1 = [[0, 0, 0], [1, 1, 1], [1, 2, 3]].$$

The differential d of Khovanov homology hence changes the vector S accordingly. For example,

$$dS_1 = 0.$$

$$\begin{aligned} d[[0, 0, 0], [0, 0, 0], [1, 2, 3]] &= [[1, 0, 0], [0, 0], [1, 3]] \\ &+ [[0, 1, 0], [0, 0], [1, 2]] + [[0, 0, 1], [0, 0], [1, 2]]. \end{aligned}$$

We consider Khovanov chain complex as a graded \mathbb{Z} -module of finite ranks, then a differential can be viewed as \mathbb{Z} -valued matrix. In fact, the matrix has entry only ± 1 and 0. Then using Gaussian elimination, all matrices can be simplified. By comparing the ranks of kernels and images, the rank of Khovanov homology at each grading can be obtained. What is in our best interest is not just the rank, but the chain complex and the unreduced differential matrices. These information will be used to compute the explicit generators

of the homology and hence the chain maps induced by the cobordisms.

B.2 Extensions to KhoHo.

There are mainly two extensions to KhoHo: one is finding the explicit generators of the Khovanov homology, another one is computing the chain maps induced by Reidemeister moves and surgeries. For convenience we work over \mathbb{Q} coefficient.

We take all the matrices of the differential before Gaussian elimination. For each grading of the Khovanov chain complex, we have a finite dimensional vector space. Each differential is a binary matrix. Take the kernel of the differential, we have a collection of column vectors which are cycles of the chain complex. Suppose

$$\cdots \xrightarrow{d_0} CKh^{i,j} \xrightarrow{d_1} CKh^{i-1,j} \xrightarrow{d_2} \cdots$$

Let $\ker d_2 = \{v_1, v_2, \dots, v_n\}$, where v_i is a column vector, which is a $(i - 1, j)$ -cycle of the chain complex. Suppose the rank of d_1 is m_0 , let $M = d_1$. Concatenate v_1 and M to get a new matrix T . Compare the rank of T and M , if the rank of T is larger, then let $M = T$, otherwise, skip v_1 and concatenate M and v_2 and so on until the rank of M equals $r + m_0$ where r is the rank of $Kh^{i-1,j}$. The last r column of M will be the generators of

Khovanov homology. The algorithm is summarized below.

```

1 count=0; /* counting variable */
2 i = 1;
3 M = d[1];
4 while count<r
5     T=[M,v[j]]; /* concatnate M and v[j] */
6
7     /* check if v[j] is in the image of M */
8     if rank(T) > rank(M)
9         M =T;
10        count++;
11        j++;
12        if j>n
13            break;

```

Eventually we will have a collection of generators of the homology, which is a linear combination of enhanced states, whose coefficients are in fact integers.

The implementation is shown below.

```

1 find_H_gens (prepD , i_deg , j_deg )=
2 {
3     local (d1 , d2 , j_matr , i_matr , ker , ker_rank , im_rank );
4     local (Kh_gens_s , cnt , H_rank , b , nonzero , ker_temp , t );
5
6     /* Initialize the differential matrices to obtain alldiff ,
7      * chain_ranks and betti numbers */
8     Betti (prepD );
9

```

```

10  /* Initialize the matrix for homology generators*/
11
12  j_matr=j2m(prexD , j_deg);
13  i_matr=i2m(prexD , i_deg);
14
15  H_rank=Betti(prexD)[j_matr , i_matr];
16  Kh_gens_s=vector(H_rank , b , []);
17
18  /* alldiff restore all information of differential matrices */
19
20  if(i_deg<prexD.iHigh ,
21      d2=alldiff[j_matr , i_matr] , d2=[;]);
22
23  if(i_deg>prexD.iLow ,
24      d1=reduce_mat( alldiff[j_matr , i_matr-1] ) , d1=[;]);
25
26  if(d2==0||d2==[;],
27
28      /* if d2=0, kernel is everything ,
29      * represented by id matrix */
30      ker=matid(chain_ranks[j_matr , i_matr]);
31      ker_rank=chain_ranks[j_matr , i_matr]; ,
32
33      ker=matkerint(Mat(d2));
34      ker_rank=length(ker);
35  );
36  /* Order ker in the way that the number *

```

```

37      * of nonzero entry in each column is increasing */
38
39      ker_temp=ker;
40      t=vecsort(vector(ker_rank , i , length(t2s(ker[,i])[1,]))
41                ,,1);
42
43      for(a=1,ker_rank ,
44          ker[,a]=ker_temp[,t[a]]
45          );
46      /*Find the rank of the image of d1 */
47
48      if(d1==[;]||d1==0,im_rank=0;d1=[;];
49          ,im_rank=length(d1));
50      cnt=0;
51      a=1;
52
53      while(a<=ker_rank && cnt<H_rank ,
54          if(length(mathnf(concat(d1 , ker[,a]))) > (im_rank+cnt) ,
55              cnt++;
56              d1=concat(d1 , ker[,a]);
57              nonzero = [];
58
59              for(b=1,length(ker[,a]) ,
60                  if(ker[b,a]!=0 , nonzero=concat(nonzero ,[b]))
61                  );
62              Kh_gens_s[cnt]=matrix(2 , length(nonzero));

```

```

63         Kh_gens_s [ cnt ] [ 1 , ] = vecextract ( ker [ , a ] ~ , nonzero );
64         Kh_gens_s [ cnt ] [ 2 , ] = nonzero ;
65     ) ;
66     a ++ ;
67 ) ;
68
69     /* Check if j-deg or i-deg exceed the bound. */
70     j = ( prepD . jHigh - j_deg ) / 2 + 1 ;
71     if ( ( j > matsize ( chain_ranks ) [ 1 ] - 1 ) ||
72         ( i_matr == matsize ( chain_ranks ) [ 2 ] ) ,
73         Kh_gens_s = [ ; ] ) ;
74     return ( Kh_gens_s ) ;
75 }

```

Chain maps induced by Reidemeister moves and 1-surgery are defined explicitly by different authors, for example, Bar-Natan [1]. Our computation for chain maps are based on an equivalent definition. First of all, since the computation of the program is based on the diagram, we need to know how the link diagram changes under all Reidemeister moves and 1-surgery. Since the link diagram is represented by a matrix, we need a map from the old matrix to the new one, which specifies the image of each entry of the matrix. Moreover, for Reidemeister move 1 and 2, the number of crossings changes as well, so we need to add or remove rows of the diagram matrix accordingly. The code below is for changes the diagram matrix under the first Reidemeister move.

```

1 R1_diagr ( prepD , edge_info , config ) =

```

```

2 {
3   local (k,x,D,R1_D,i,j,name,xnum);
4   k=edge_info [1];
5   xnum=prepD.vnum;
6
7   if (config [1]>0,
8     if (config == [1,1,1],
9       R1_D=concat (prepD [1] , [k,k+2,k+1,k+1]);
10      name="R1_OU_");
11
12    if (config == [1,1,0],
13      R1_D=concat (prepD [1] ,
14        /* "order" is an auxiliary function that reorder
15         * the first vector according to the permutation
16         * that make the second vector in ascending order. */
17        order ([k,k+2,k+1,k+1] , [1,4,3,2]) [1]);
18      name="R1_OD_");
19
20    if (config == [1,0,1],
21      R1_D=concat (prepD [1] ,
22        order ([k,k+2,k+1,k+1] , [2,3,1,4]) [1]);
23      name="R1_OD_");
24
25    if (config == [1,0,0],
26      R1_D=concat (prepD [1] ,
27        order ([k,k+2,k+1,k+1] , [4,3,2,1]) [1]);
28      name="R1_UD_");

```

```

29
30     for (i=1, xnum,
31         for (j=1,4,
32             if ((prepD [1][i,j]==k &&
33                 (j==1 || (j%2==0
34                     && (prepD [1][i,6-j]-k==1
35                         || k-prepD [1][i,6-j]>1
36                             )
37                     )
38                 )
39             ) || prepD [1][i,j]>k,
40
41                 R1_D[i,j]=prepD [1][i,j]+2;
42             );
43         );
44     );
45 );
46
47 /* the config for inverse map is different.
48 * It tells the information of the entering edge.
49 * config[1] tells it is inverse or not,
50 * config[2] tells positive or negative kink,
51 * 0 for positive, config[3] tells orientation,
52 * 1 for up, 0 for down */
53 if (config [1]<0,
54     R1_D=vecextract (prepD [1],
55                     vector (xnum-1,i,i),

```

```

56         vector(4,i,i)
57     );
58
59     x=locate_crossing(prexD[1],edge_info);
60     D=prexD[1][x[1],];
61     if(config==[-1,0,1], name="R1-PU");
62     if(config==[-1,0,0], name="R1-PD");
63     if(config==[-1,1,1], name="R1-NU");
64     if(config==[-1,1,0], name="R1-ND");
65
66     for(i=1, xnum-1,
67         for(j=1,4,
68             R1_D[i,j]=new_ed(D,vecextract(config,[2,3]),
69                 prepD[1][i,j]
70                 );
71         );
72     );
73 );
74
75 check_diagr(R1_D);
76 return(prelink(R1_D,Str(name,prexD[2])));
77 }

```

We can also compute how each enhanced state changes and hence how the generator of the homology changes. To compute the surface invariant $\mathcal{M}(F)$, we start with one diagram matrix, after several moves, we end up with the same link diagram but different diagram matrix. To compute the

action under these moves, we need one more step which is transferring the new diagram matrix back to the starting diagram matrix, so that we obtain a matrix by converting the transformed generator to a linear combination of the original generators. The code below is for changing a generator under a local move and obtaining the transformation matrix.

```

1 R_gens (prepD , move_type , all_gens )=
2 {
3     local (xnum,x,R,D, config , gens , new_gens );
4     local ( i ,p,l , deg_i , deg_j , temp_states , new_states );
5     xnum=prepD.vnum;
6
7     if (move_type[1]==3, config = [move_type [3]]; ,
8         config=move_type [3]);
9
10    if (config [1]<0 || move_type [1]==3,
11        x=locate_crossing (prepD [1] , move_type [2]);
12        if (move_type [1]==2,
13            x=concat (x, locate_crossing (prepD [1] ,
14                [prepD [1] [x [1] ,3]))
15                );
16        );
17        tempD=prelink (move2end (prepD [1] , x) , prepD [2]); ,
18
19        tempD=prepD;
20    );
21
22    if (move_type [1]==1,

```



```

23         R_D=R1_diagr(tempD,move_type[2],config);
24     );
25
26     if(move_type[1]==2,
27         R_D=R2_diagr(tempD,move_type[2],config);
28     );
29
30     if(move_type[1]==3,
31         R_D=R3_diagr(tempD,move_type[2],move_type[3]);
32     );
33
34     list_generators(R_D);
35     New_Info=states_info;
36     list_generators(tempD);
37     Old_Info=states_info;
38
39     if(all_gens==[],
40         list_all_H_gens(prexD);
41         gens=H_gens; ,
42
43         gens=all_gens;
44     );
45
46     new_gens=vector(length(gens),i,
47         [gens[i][1],vector(length(gens[i][2]),p,[])])
48     );
49

```

```

50 for(i=1, length(gens),
51     deg_i=gens[i][1][1];
52     deg_j=gens[i][1][2];
53     for(p=1, length(gens[i][2]),
54         if(all_gens==[],
55             temp_states=
56                 vector(length(gens[i][2][p][2,]), i, []);
57             for(l=1, length(gens[i][2][p][2,]),
58                 n=gens[i][2][p][2,1];
59                 temp_states[1]=concat(gens[i][2][p][1,1],
60                     recover_state(prexD, deg_i, deg_j, n));
61                 temp_states[1][4]=Vec(temp_states[1][4]);
62             );
63
64             if(length(gens[i][2][p][1])==4,
65                 temp_states=gens[i][2][p];,
66                 temp_states=gens[i][2];
67             );
68         );
69
70         if(move_type[1]==1,
71             new_gens[i][2][p]=
72                 R1_gen(prexD, R_D, move_type[2],
73                     config, temp_states);
74         );
75
76         if(move_type[1]==2,

```

```

77     new_gens[i][2][p]=
78         R2_gen(prexD, R.D, move_type[2],
79             config, temp_states);
80 );
81
82     if(move_type[1]==3,
83         new_gens[i][2][p]=
84             R3_gen(prexD, R.D, move_type[2], move_type[3],
85                 temp_states);
86     );
87 );
88     while(length(new_gens[i][2][1])==1
89         && length(new_gens[i][2])==1,
90         new_gens[i][2]=new_gens[i][2][1];
91     );
92
93     while(length(new_gens[i])==1,
94         new_gens[i]=new_gens[i][1]);
95 );
96 return([R.D, new_gens]);
97 }
98
99 R_mat(prexD1, prexD2, img, p, i_deg, j_deg, gens)=
100 {
101     local(xnum, cmp1, cmp2, i, j, k, s, trf_gens, sp_gens, mat);
102     xnum=prexD1[3];
103     trf_gens=gens;

```

```

104  cmp1=find_cmpo (prepD1);
105  cmp2=find_cmpo (prepD2);
106  binvec2num = vectorv(xnum, i, 2 ^ (i - 1));
107
108  for(i=1, length(gens),
109      if(type(gens[i][1])=="t_INT", gens[i]=[gens[i]]);
110      trf_gens[i]=gens[i];
111      for(j=1, length(gens[i]),
112          gen=gens[i][j];
113          temp=trf_state(gen[2],p);
114          trf_gens[i][j][1]=temp[1]*gen[1];
115          trf_gens[i][j][2]=temp[2];
116          s = trf_gens[i][j][2]* binvec2num + 1;
117          new_info=New_Info[s];
118          temp=trf_edge(cmp1,cmp2,img,gen[4]);
119          trf_gens[i][j][4]=
120          vector(length(temp),k,
121              new_info[4][new_info[3][temp[k]]]
122          );
123          trf_gens[i][j][3]=order(gen[3],
124              trf_gens[i][j][4])[1];
125          trf_gens[i][j][4]=vecsort(trf_gens[i][j][4],,2);
126      );
127
128  sp_gens=vector(length(gens));
129  for(i=1, length(gens),
130      sp_gens[i]=matrix(2,length(gens[i]));

```

```

131         for(j=1, length(gens[i]),
132             sp-gens[i][1,j]=trf-gens[i][j][1];
133             sp-gens[i][2,j]=
134             recover-gen(prexD2,i-deg,j-deg,
135                         vecextract(trf-gens[i][j],[2,3])
136                                 );
137         );
138     );
139     mat=transf-mat(prexD2,i-deg,j-deg,sp-gens);
140     return(mat);
141 }

```

Appendix C

Some Computational Results

For Knot(5,1) and Knot(7,1), the result is just the Khovanov homology of the knot with rotation acting by identity. For Borromean Ring as in Figure C.1 and Knot(10, 123) as in ¹Figure C.2, the results are different.

Let F_B be the surface obtained by rotating the Borromean ring around the imaginary center of the diagram and closed up by gluing the two ends. Then

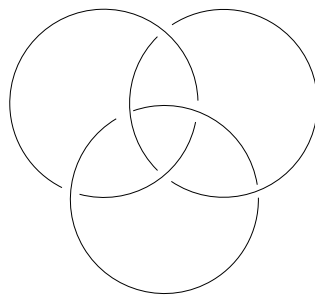


Figure C.1: Borromean Ring

¹The figure of Knot(10,123) is from http://katlas.org/wiki/10_123

$$\mathcal{M}^{i,j}(F_t) \cong \begin{cases} R/(t-1) & (i,j) = \pm(2,3), \pm(3,7) \\ R/(t^2+t+1) & (i,j) = \pm(2,5), \pm(1,1) \\ R/(t^3-1) \oplus R/(t-1) & (i,j) = (0, \pm 1) \\ 0 & \text{otherwise} \end{cases}$$

Let F_S be the surface obtained by rotating the Knot(10,123) around the imaginary center of the diagram and closed up by gluing the two ends.

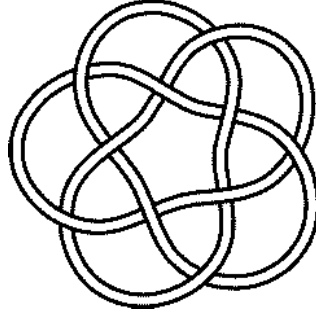


Figure C.2: Knot(10,123)

$$\mathcal{M}^{i,j}(F_S) \cong \begin{cases} R/(t-1) & (i,j) = \pm(4,7), \pm(5,11) \\ R/(t^4+t^3+t^2+t+1) & (i,j) = \pm(4,9), \pm(3,5) \\ R/(t^5-1) & (i,j) = \pm(3,7) \\ R/(t^5-1) \oplus R/(t^4+t^3+t^2+t+1) & (i,j) = \pm(2,5), \pm(1,1) \\ R/(t^5-1) \oplus R/(t-1) & (i,j) = \pm(2,3) \\ R/(t^5-1) \oplus R/(t^5-1) & (i,j) = \pm(1,3) \\ R/(t^5-1) \oplus R/(t^5-1) \oplus R/(t-1) & (i,j) = (0, \pm 1) \\ 0 & \text{otherwise} \end{cases}$$

Knots or links with more crossings (> 10) are not computed due to the computational complexity.

Appendix D

Calculations on the Third Reidemeister Moves

Our calculation is based on the Gaussian elimination Lemma in [2] which states the following:

Lemma D.0.1. (*Double Gaussian Elimination*) Consider the chain complex

$$\begin{array}{ccccccc}
 & & & & D_1 & & \\
 & & B & & \oplus & & F \\
 A & \xrightarrow{\begin{pmatrix} \bullet \\ \alpha \end{pmatrix}} & \oplus & \xrightarrow{\begin{pmatrix} \psi & \beta \\ \gamma & \delta \end{pmatrix}} & D_2 & \xrightarrow{\begin{pmatrix} \bullet & \varphi & \lambda \\ \bullet & \mu & \nu \end{pmatrix}} & \oplus & \xrightarrow{\begin{pmatrix} \bullet \\ \eta \end{pmatrix}} & H \\
 & & C & & \oplus & & G \\
 & & & & E & &
 \end{array}$$

in an additive category, where $\psi : B \rightarrow D_1$ and $\varphi : D_2 \rightarrow F$ are isomor-

morphisms, and all other morphisms including \bullet are arbitrary morphisms. Then there is a homotopy equivalence between this complex and a much simpler complex:

$$\begin{array}{ccccccc}
 & & & D_1 & & & \\
 & & B & \oplus & F & & \\
 A & \xrightarrow{(\bullet \cdot \alpha)} & \oplus & \xrightarrow{\begin{pmatrix} \psi & \beta \\ \gamma & \delta \end{pmatrix}} & \oplus & \xrightarrow{\begin{pmatrix} \bullet & \varphi & \lambda \\ \mu & \nu \end{pmatrix}} & \oplus & \xrightarrow{(\bullet \cdot \eta)} & H \\
 & & C & \oplus & G & & & & \\
 \uparrow & & \uparrow & \oplus & \uparrow & & \uparrow & & \uparrow \\
 (1) & & (0 \ 1) & & (-\mu\varphi^{-1} \ 1) & & (0 \ 1) & & (1) \\
 & & \begin{pmatrix} -\psi^{-1} & \beta \\ & 1 \end{pmatrix} & \begin{pmatrix} -\gamma\psi^{-1} & 0 & 1 \end{pmatrix} & \begin{pmatrix} 0 & \\ -\varphi^{-1} & \lambda \end{pmatrix} & & & & \\
 A & \xrightarrow{(\alpha)} & C & \xrightarrow{(\delta - \gamma\psi^{-1}\beta)} & E & \xrightarrow{(\nu - \mu\varphi^{-1}\lambda)} & G & \xrightarrow{(\eta)} & H \\
 & & & & \begin{pmatrix} -\psi^{-1} & \beta \\ & 1 \end{pmatrix} & & & &
 \end{array}$$

Proof. This is Lemma A.2 in [2]. \square

Now we apply Lemma D.0.1 to the Khovanov chain complexes of both sides of the third Reidemeister move in Figure D.1. The calculation is also very similar to the one in the Appendix A.2 [2], except we don't have to worry about orientations and disorientations of the enhanced states.

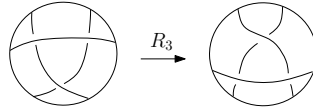


Figure D.1: The third Reidemeister move with one arc sliding over the rest.

On the left-hand-side, an ordering is fixed. There is an explicit chain map H_l which maps the chain complex on the first row to second, which is

simplified.

$$\begin{array}{ccccc}
 \begin{array}{c} \text{Diagram 1} \\ \text{Diagram 2} \end{array} & \xrightarrow{\begin{pmatrix} \psi_l \\ \gamma_{l1} \\ \gamma_{l2} \end{pmatrix}} & \begin{array}{c} \text{Diagram 3} \\ \oplus \\ \text{Diagram 4} \end{array} & \xrightarrow{\begin{pmatrix} \varphi_l & \lambda_l & 0 \\ \mu_l & 0 & \nu_{l3} \\ 0 & \nu_{l1} & \nu_{l2} \end{pmatrix}} & \begin{array}{c} \text{Diagram 5} \\ \oplus \\ \text{Diagram 6} \end{array} & \xrightarrow{(\bullet \ \eta_{l1} \ \eta_{l2})} & \begin{array}{c} \text{Diagram 7} \\ \oplus \\ \text{Diagram 8} \end{array} \\
 \downarrow \begin{pmatrix} -\gamma_{l1}\varphi_l^{-1} & 1 & 0 \\ -\gamma_{l2}\varphi_l^{-1} & 0 & 1 \end{pmatrix} & & \uparrow \begin{pmatrix} -\varphi_l^{-1}\lambda_l & 0 \\ 1 & 0 \\ 0 & 1 \end{pmatrix} & & \downarrow \begin{pmatrix} -\mu_l\varphi_l^{-1} & 1 & 0 \\ 0 & 0 & 1 \end{pmatrix} & & \downarrow (1) \\
 0 & \longrightarrow & \begin{array}{c} \text{Diagram 9} \\ \oplus \\ \text{Diagram 10} \end{array} & \xrightarrow{\begin{pmatrix} -\mu_l\varphi_l^{-1}\lambda_l & \nu_{l3} \\ \nu_{l1} & \nu_{l2} \end{pmatrix}} & \begin{array}{c} \text{Diagram 11} \\ \oplus \\ \text{Diagram 12} \end{array} & \xrightarrow{(\bullet \ \eta_{l1} \ \eta_{l2})} & \begin{array}{c} \text{Diagram 13} \\ \oplus \\ \text{Diagram 14} \end{array}
 \end{array}$$

The differentials of Khovanov chain complex are of matrix form. The entries are maps from one enhanced state to another. The Greek letters are chosen intentionally to match the Greek letters in Lemma D.0.1. The letters λ_l , ν_l and η_l in the lemma are also matrices in our case.

$$\lambda_l = \begin{pmatrix} \lambda_{l1} \\ \lambda_{l2} \end{pmatrix}, \quad \nu_l = \begin{pmatrix} 0 & \nu_{l3} \\ \nu_{l1} & \nu_{l2} \end{pmatrix}$$

and $\eta = (\eta_{l1}, \eta_{l2})$. 1 is understood as an identity matrix.

Similarly, we apply Lemma D.0.1 to the right-hand-side in Figure D.1

which gives another chain map H_r from top to bottom.

$$\begin{array}{ccccccc}
 & & & \begin{array}{c} \text{Diagram 1} \\ \oplus \\ \text{Diagram 2} \end{array} & \xrightarrow{\begin{pmatrix} \psi_r \\ \gamma_{r1} \\ \gamma_{r2} \end{pmatrix}} & \begin{array}{c} \text{Diagram 1} \\ \oplus \\ \text{Diagram 2} \end{array} & \xrightarrow{\begin{pmatrix} \varphi_r & \lambda_r & 0 \\ \mu_r & 0 & \nu_{r3} \\ 0 & \nu_{r1} & \nu_{r2} \end{pmatrix}} & \begin{array}{c} \text{Diagram 1} \\ \oplus \\ \text{Diagram 2} \end{array} & \xrightarrow{(\bullet \eta_{r1} \eta_{r2})} & \text{Diagram 3} \\
 & & & \downarrow & & \downarrow & & \downarrow & & \downarrow & \\
 & & & \begin{pmatrix} -\gamma_{r1}\varphi_r^{-1} & 1 & 0 \\ -\gamma_{r2}\varphi_r^{-1} & 0 & 1 \end{pmatrix} & & \begin{pmatrix} -\mu_r\varphi_r^{-1} & 1 & 0 \\ 0 & 0 & 1 \end{pmatrix} & & \begin{pmatrix} 0 & 0 \\ 1 & 0 \\ 0 & 1 \end{pmatrix} & & (1) & \\
 & & & \uparrow & & \uparrow & & \uparrow & & \uparrow & \\
 0 & \longrightarrow & \begin{array}{c} \text{Diagram 1} \\ \oplus \\ \text{Diagram 2} \end{array} & \xrightarrow{\begin{pmatrix} -\mu_r\varphi_r^{-1}\lambda_r & \nu_{r3} \\ \nu_{r1} & \nu_{r2} \end{pmatrix}} & \begin{array}{c} \text{Diagram 1} \\ \oplus \\ \text{Diagram 2} \end{array} & \xrightarrow{(\bullet \eta_{r1} \eta_{r2})} & \text{Diagram 3} & & & &
 \end{array}$$

By comparing the reduced complex of both sides, we can see that there is a natural isomorphism between them. In fact, this isomorphism identifies

states with the same smoothing.

$$\begin{array}{ccccc}
 \begin{array}{c} \text{Diagram 1} \\ \oplus \\ \text{Diagram 2} \end{array} & \xrightarrow{\begin{pmatrix} -\mu_l \varphi_l^{-1} \lambda & \nu_{l3} \\ \nu_{l1} & \nu_{l2} \end{pmatrix}} & \begin{array}{c} \text{Diagram 3} \\ \oplus \\ \text{Diagram 4} \end{array} & \xrightarrow{(\bullet \eta_{l1} \eta_{l2})} & \text{Diagram 5} \\
 \uparrow (1) & & \begin{array}{c} \left(\begin{array}{cc} 0 & 1 \\ 1 & 0 \end{array} \right) \\ \updownarrow \\ \left(\begin{array}{cc} 0 & 1 \\ 1 & 0 \end{array} \right) \end{array} & & \uparrow (1) \\
 \begin{array}{c} \text{Diagram 6} \\ \oplus \\ \text{Diagram 7} \end{array} & \xrightarrow{\begin{pmatrix} -\mu_r \varphi_r^{-1} \lambda_r & \nu_{r3} \\ \nu_{r1} & \nu_{r2} \end{pmatrix}} & \begin{array}{c} \text{Diagram 8} \\ \oplus \\ \text{Diagram 9} \end{array} & \xrightarrow{(\bullet \eta_{r1} \eta_{r2})} & \text{Diagram 10}
 \end{array}$$

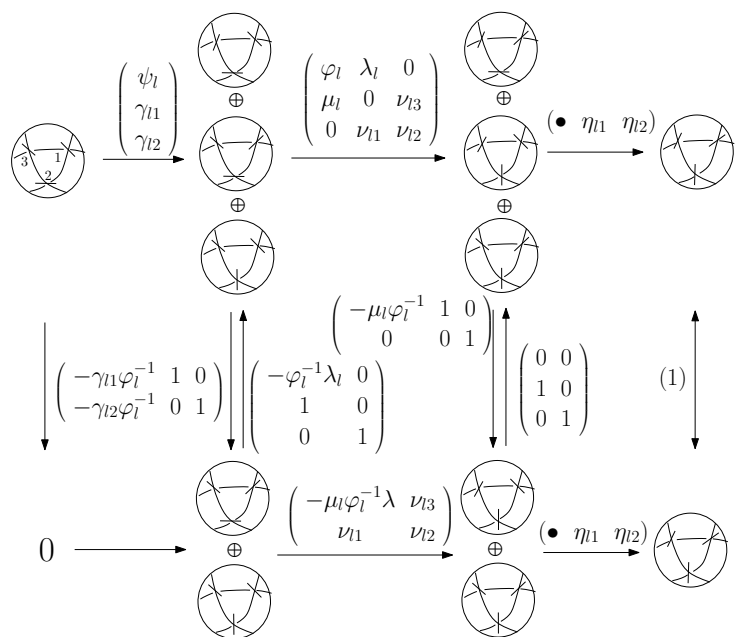
This isomorphism together with H_l and H_r defines a homotopy equivalence between the Khovanov chain complex of two sides of Figure D.1. The result is summarized on the left in Figure 6.15.

On the other hand, we do the same calculation for another version of the third Reidemeister move. We apply Lemma D.0.1 to the left-hand-side of

$$\begin{array}{c} \text{Diagram 11} \end{array} \xrightarrow{(R_3)'} \begin{array}{c} \text{Diagram 12} \end{array}$$

Figure D.2: The third Reidemeister move with one arc sliding under the rest.

Figure D.2:



On the right-hand-side, we have

$$\begin{array}{ccccccc}
 \begin{array}{c} \text{Diagram 1} \\ \text{Diagram 2} \\ \text{Diagram 3} \end{array} & \xrightarrow{\begin{pmatrix} \psi_r \\ \gamma_{r1} \\ \gamma_{r2} \end{pmatrix}} & \begin{array}{c} \text{Diagram 4} \\ \oplus \\ \text{Diagram 5} \\ \oplus \\ \text{Diagram 6} \end{array} & \xrightarrow{\begin{pmatrix} \varphi_r & \lambda_r & 0 \\ \mu_r & 0 & \nu_{r3} \\ 0 & \nu_{r1} & \nu_{r2} \end{pmatrix}} & \begin{array}{c} \text{Diagram 7} \\ \oplus \\ \text{Diagram 8} \\ \oplus \\ \text{Diagram 9} \end{array} & \xrightarrow{(\bullet \eta_{r1} \eta_{r2})} & \begin{array}{c} \text{Diagram 10} \\ \text{Diagram 11} \end{array} \\
 \downarrow \begin{pmatrix} -\gamma_{r1}\varphi_r^{-1} & 1 & 0 \\ -\gamma_{r2}\varphi_r^{-1} & 0 & 1 \end{pmatrix} & & \updownarrow \begin{pmatrix} -\varphi_r^{-1}\lambda_r & 0 \\ 1 & 0 \\ 0 & 1 \end{pmatrix} & & \updownarrow \begin{pmatrix} -\mu_r\varphi_r^{-1} & 1 & 0 \\ 0 & 0 & 1 \end{pmatrix} & & \updownarrow \begin{pmatrix} 0 & 0 \\ 1 & 0 \\ 0 & 1 \end{pmatrix} & & \updownarrow (1) \\
 0 & \longrightarrow & \begin{array}{c} \text{Diagram 12} \\ \oplus \\ \text{Diagram 13} \end{array} & \xrightarrow{\begin{pmatrix} -\mu_r\varphi_r^{-1}\lambda_r & \nu_{r3} \\ \nu_{r1} & \nu_{r2} \end{pmatrix}} & \begin{array}{c} \text{Diagram 14} \\ \oplus \\ \text{Diagram 15} \\ \oplus \\ \text{Diagram 16} \end{array} & \xrightarrow{(\bullet \eta_{r1} \eta_{r2})} & \begin{array}{c} \text{Diagram 17} \\ \text{Diagram 18} \end{array}
 \end{array}$$

We compare the reduced complexes:

$$\begin{array}{ccccccc}
 \begin{array}{c} \text{Diagram 19} \\ \oplus \\ \text{Diagram 20} \end{array} & \xrightarrow{\begin{pmatrix} -\mu_l\varphi_l^{-1}\lambda & \nu_{l3} \\ \nu_{l1} & \nu_{l2} \end{pmatrix}} & \begin{array}{c} \text{Diagram 21} \\ \oplus \\ \text{Diagram 22} \end{array} & \xrightarrow{(\bullet \eta_{l1} \eta_{l2})} & \begin{array}{c} \text{Diagram 23} \\ \text{Diagram 24} \end{array} \\
 \updownarrow (1) & & \updownarrow \begin{pmatrix} 0 & 1 \\ 1 & 0 \end{pmatrix} & & \updownarrow (1) \\
 \begin{array}{c} \text{Diagram 25} \\ \oplus \\ \text{Diagram 26} \end{array} & \xrightarrow{\begin{pmatrix} -\mu_r\varphi_r^{-1}\lambda_r & \nu_{r3} \\ \nu_{r1} & \nu_{r2} \end{pmatrix}} & \begin{array}{c} \text{Diagram 27} \\ \oplus \\ \text{Diagram 28} \\ \oplus \\ \text{Diagram 29} \end{array} & \xrightarrow{(\bullet \eta_{r1} \eta_{r2})} & \begin{array}{c} \text{Diagram 30} \\ \text{Diagram 31} \end{array}
 \end{array}$$

Again we can use the identification above together with the chain maps

obtained earlier to construct a chain map the this version of the Third Reidemeister move. The result is summarized on the right in Figure 6.15.

For other variation of the third Reidemeister moves, the computations are the same. See the result in Figure 6.16.

Notice that the chain maps induced by the third Reidemeister moves are unique only up to homotopy. We can use the chain map constructed for Figure D.1 to define a chain map for Figure D.2. In fact, in Figure D.3, sliding the thick arc under a crossing is the same as sliding the thick arc over the crossing, the latter of which is exactly the version in Figure D.1.

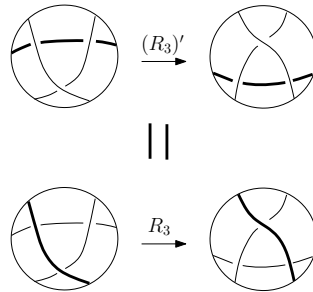


Figure D.3: Slide the thick arc under a crossing is the same as slide the thick arc over the crossing.

It is not difficult to prove that the chain map obtained this way is different from the one we constructed using Lemma D.0.1, but they are chain homotopic. In fact, it is proved in several papers ([1], [2] and so on) that the chain maps induced by Reidemeister moves are unique up to chain homotopy. Thus we can choose an alternative chain map for our purpose.